Investigating HMGB1 as a Potential Serum Biomarker for Early Diabetic Nephropathy Monitoring by Quantitative Proteomics

Rui Peng, Siyang Zuo, Xia Li, Yun Huang, Siyu Chen, Xue Zou, Hehua Long, Min Chen, Yuan Yang, Huixiong Yuan, Qingqing Zhao, Bing Guo, Lirong Liu

PII: S2589-0042(24)00055-5

DOI: https://doi.org/10.1016/j.isci.2024.108834

Reference: ISCI 108834

To appear in: ISCIENCE

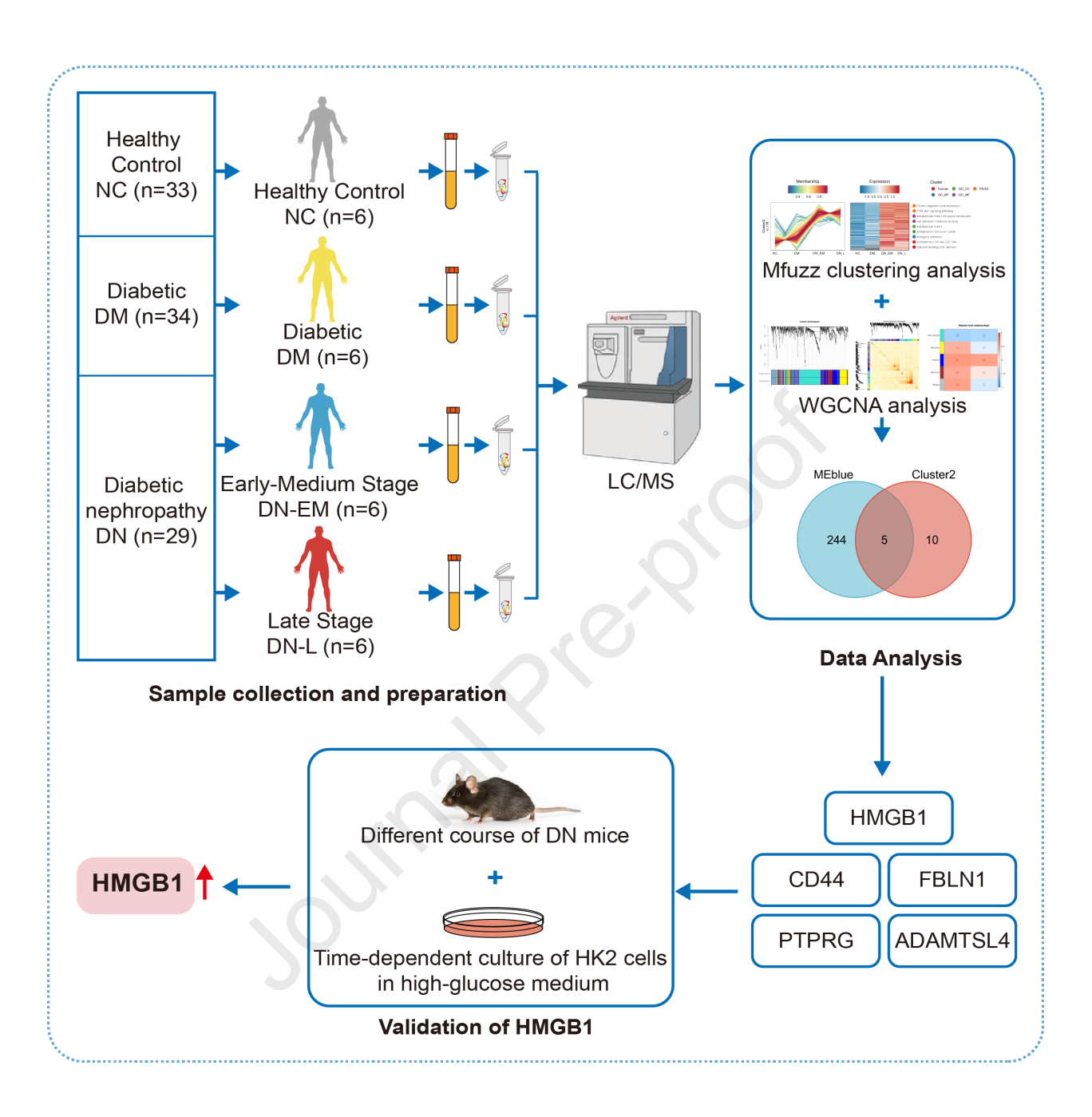
Received Date: 1 September 2023
Revised Date: 1 December 2023
Accepted Date: 3 January 2024

Please cite this article as: Peng, R., Zuo, S., Li, X., Huang, Y., Chen, S., Zou, X., Long, H., Chen, M., Yang, Y., Yuan, H., Zhao, Q., Guo, B., Liu, L., Investigating HMGB1 as a Potential Serum Biomarker for Early Diabetic Nephropathy Monitoring by Quantitative Proteomics, *ISCIENCE* (2024), doi: https://doi.org/10.1016/j.isci.2024.108834.

This is a PDF file of an article that has undergone enhancements after acceptance, such as the addition of a cover page and metadata, and formatting for readability, but it is not yet the definitive version of record. This version will undergo additional copyediting, typesetting and review before it is published in its final form, but we are providing this version to give early visibility of the article. Please note that, during the production process, errors may be discovered which could affect the content, and all legal disclaimers that apply to the journal pertain.

© 2024





1 Investigating HMGB1 as a Potential Serum Biomarker for Early

Diabetic Nephropathy Monitoring by Quantitative Proteomics

- 3 Rui Peng,^{1,2,3} Siyang Zuo,^{1,2,3} Xia Li,^{3,6} Yun Huang¹, Siyu Chen,^{1,2,3} Xue Zou,⁶ Hehua
- 4 Long, 1,2,3 Min Chen, 1,2,3 Yuan Yang, 1,2,3 Huixiong Yuan, 1,2,3 Qingqing Zhao, 6 Bing
- 5 Guo,^{4,5} and Lirong Liu^{1,2,3,7,*}
- 6 ¹ Center for Clinical Laboratories, the Affiliated Hospital of Guizhou Medical
- 7 University, Guiyang, 550004, China
- 8 ² School of Clinical Laboratory Science, Guizhou Medical University, Guiyang,
- 9 550004, China
- ³ Guizhou Precision Medicine Institute, the Affiliated Hospital of Guizhou Medical
- 11 University, Guiyang, 550004, China
- ⁴ Department of Pathophysiology, Guizhou Medical University, Guiyang, 550025,
- 13 China
- ⁵ Laboratory of Pathogenesis Research, Drug Prevention and Treatment of Major
- Diseases, Guizhou Medical University, Guiyang, 550025, China
- ⁶ Center for Clinical Medical Research, the Affiliated Hospital of Guizhou Medical
- 17 University, Guiyang, 550004, China
- 18 ⁷ Lead contact

19 *Corresponding Authors:

20 Lirong Liu, Email: lirongliu@gmc.edu.cn.

21

SUMMARY

1

Current diagnostic methods for diabetic nephropathy (DN) lack precision, especially in 2 early stages and monitoring progression. This study aims to find potential biomarkers 3 for DN progression and evaluate their accuracy. Using serum samples from healthy 4 controls (NC), diabetic patients (DM), early-medium stage DN (DN-EM), and late-5 stage DN (DN-L), researchers employed quantitative proteomics and Mfuzz clustering 6 7 analysis revealed 15 proteins showing increased expression during DN progression, hinting at their biomarker potential. Combining Mfuzz clustering with weighted gene 8 co-expression network analysis (WGCNA) highlighted five candidates (HMGB1, 9 CD44, FBLN1, PTPRG, and ADAMTSL4). HMGB1 emerged as a promising 10 biomarker, closely correlated with renal function changes. Experimental validation 11 12 supported HMGB1's upregulation under high glucose conditions, reinforcing its potential as an early detection biomarker for DN. This research advances DN 13 understanding and identifies five potential biomarkers, notably HMGB1, as a 14 promising early monitoring target. These findings set the stage for future clinical 15 16 diagnostic applications in DN.

17

1 INTRODUCTION

Diabetes mellitus (DM) is a chronic metabolic disease characterized by chronic 2 hyperglycemia caused by impaired insulin secretion or utilization. Globally, over 415 3 million people suffer from DM, and 693 million are expected to be diagnosed with it 4 by 2045 ¹. Diabetes nephropathy (DN) is one of the major microvascular complications 5 of DM, and approximately 30%-40% of patients with DM will develop DN ². 6 Unfortunately, the majority of DN patients progress without symptoms until they 7 develop renal injury and then irreversible renal failure, which is treated only with 8 kidney transplantation and dialysis. Besides posing a threat to patients' lives, DN is 9 also an enormous economic and medical burden on patients and society³. To effectively 10 prevent and treat DN, early diagnosis is therefore crucial. 11 Renal biopsy is still the golden standard for diagnosing and typing DN. Nonetheless, 12 this invasive approach has inherent limitations, such as the possibility of bleeding 13 complications and the biases in its sampling 4. Therefore, the diagnosis of DN is 14 increasingly being conducted using non-invasive surrogate techniques. Biomarkers can 15 be used to identify people with diseases and redefine disease classifications ^{5,6}. Classic 16 markers for assessing the severity of DN include proteinuria, estimated glomerular 17 filtration rate (eGFR), creatinine (Crea) and blood urea nitrogen (BUN) ^{7,8}. These 18 biomarkers accurately quantify the degree of renal injury in patients with DN, but they 19 20 don't have sufficient accuracy to discern the mild renal insufficiency of early DN. It is now widely accepted that albuminuria, a protein that is filtered through the glomerulus 21 and then reabsorbed by the renal tubules, can monitor the development of DN 9. 22 However, 20-40% of DM patients already have an eGFR decline before they are 23 detected with albuminuria ¹⁰. Furthermore, the precise role of novel biomarkers such as 24 microRNA (miRNA), long noncoding RNA (lncRNA), and urinary exosomes in DN 25 still remains to be determined 11. Therefore, DN management requires non-invasive or 26 minimally invasive methods that are more sensitive and selective for the detection of 27 DN as well as monitoring the progression of DN. 28

1	Proteomics based on mass spectrometry (MS) is the technology of choice for analyzing
2	proteins to discover potential disease-related biomarkers ^{12,13} . Serum contains
3	numerous secreted proteins that play crucial roles in physiological and pathological
4	changes ¹⁴ . Therefore, comprehensive serum proteomics can be used to discover novel
5	protein biomarkers for DN that may be obtained to learn more about pathophysiology
6	and increase the accuracy of diagnostic stratification. Despite numerous studies
7	exploring serum proteomics for potential DN biomarkers, the detection of only a
8	limited number of proteins has been predominantly attributed to methodological
9	limitations ^{15,16} . Recent, studies involving the proteomics of serum for DN progression
10	had previously been undertaken, but they were unable to distinguish DM from early
11	DN ¹⁷ . Moreover, many studies only focus on biomarkers in serum, while very few
12	studies examine molecules identified through in vitro, cell-based or animal models.
13	Thus, the biomarkers of DN progression based on serum proteomics need to be further
14	explored.
15	In this study, we investigated the serum proteome of early-medium stage and late stage
16	DN patients compared with diabetic patients and healthy control subjects. Then, we
17	clustered the associated biomarkers with a similar expressive variation trend, focusing
18	on the cluster containing rise biomarkers along with DN development. With weighted
19	gene co-expression network analyses (WGCNA) of all biomarkers, we explored which
20	of the biomarkers was most relevant for DN progression and whether it was able to
21	discriminate DN or not. We confirmed that the biomarker is elevated in both cell-based
22	and animal models of high glucose. This study identifies a potential candidate
23	biomarker to monitor the progression of DN patients and may be used in clinical
24	practice.

25

26

27

RESULTS

Participant characteristics and assessment of the serum proteome analysis

A total of 96 patients, including healthy control (NC, male/female: 11/22), diabetic 1 (DM, male/female:20/14), and diabetic nephropathy (DN, male/female: 16/13) were 2 recruited. Upon enrollment for serum proteomic analysis, patients' inclusion and 3 exclusion criteria were reset. According to the estimated glomerular filtration rate 4 (eGFR) categories in chronic kidney disease (CKD) by the Kidney Disease Improving 5 Global Outcomes (KDIGO) 18, patients were further divided into four groups (Figure 6 1A): healthy control (NC, eGFR ≥ 90 ml/min/1.73 m²), diabetic (DM, eGFR ≥ 90 7 8 ml/min/1.73 m²), early medium stage (DN-EM, $30 \le eGFR < 90 \text{ ml/min/1.73 m}^2$), and late stage (DN-L, eGFR \leq 30 ml/min/1.73 m²), with 6 patients in each group. 9 Demographic and clinical characteristics of the subjects are demonstrated in Table 1. 10 The study included 12 females and 12 males, ages 40-80, and patients in the DN-EM 11 12 and DN-L groups were older than the DM group; the observed distinction presented a statistically significant difference. No significant discrepancies were found in the 13 gender and levels of uric acid between the four groups of participants. The blood 14 glucose level in the DM, DNEM and DNL groups was significantly higher than that in 15 16 NC group. In the DN-L group, serum creatinine and cystatin c levels were significantly elevated, and the blood urea nitrogen to serum creatinine ratio was significantly lower 17 than in the NC and DM groups, while the level of blood urea nitrogen was significantly 18 higher than in the NC, DM and DNEM groups. Meanwhile, the DN-L group had a 19 20 significantly lower eGFR than the NC, DM and DNEM groups, and the DMEM group had a significantly lower eGFR than DM. 21 22 Different protein levels in serum range over large orders of magnitude and are very heterogeneous compared to tissues or cellular samples. To obtain more comprehensive 23 24 and useful proteins related to the DN pathogenesis, we filtered out the interference of high abundance proteins in serum. Subsequent, 1602 proteins were identified by 25 LC/MS, of which 1402 proteins could be quantified (Figure 1B). It was consistent with 26 the general rule based on enzymatic hydrolysis and mass spectrum fragmentation mode 27 that most peptide segments were distributed in 7-20 amino acids, indicating that the 28 distribution of peptide lengths identified by mass spectrum met quality control 29

standards (Figure 1C). In order to ensure the reliability of the serum samples and assay technique, and to confirm the statistical consistency of the quantitative outcomes, a comprehensive approach was undertaken. This involved the utilization of various methods, including Pearson's Correlation Coefficient (PCC), principal component analysis (PCA), and assessment of Relative Standard Deviation (RSD). PCC analysis showed that there were high correlations between all specimens, with correlation coefficients generally higher than 0.9 (Figure 1D). Further analysis of these proteins by PCA demonstrated that the four groups could be successfully distinguished, particularly in the NC and DM groups, where reproducibility was high within each group (Figure 1E). It is worth highlighting that the DN-EM and DN-L groups exhibited the most pronounced dissimilarity compared to the other stages. This suggests a substantial alteration in the protein expression profile during the DN stage. Quantitative repeatability of proteins in each group was acceptable as shown by the boxplot of RSD (Figure 1F). Based on quality control data, the samples exhibited high quality, and the accuracy of detection techniques indicates that any alterations observed in serum proteins may be associated with pathological disorders.

Serum proteome profiling of patients with diabetic nephropathy

Comprehensive view of proteomic changes related to DN pathogenesis, quantitative results of serum proteomics were performed differentially expressed proteins analysis (P < 0.05, FC > 1.5 and FC < 1/1.5). After pre-processing and missing value filtering, a total of 484 differential proteins were shown by the differential expressed proteins heatmap (Figure 2A). In the cluster heat map, most NC and DM groups had the same pattern of differentially expressed proteins, whereas the DN-EM and DN-L groups had the same pattern. In addition, we analyzed the volcano plots of pairwise comparisons between NC, DM, DN-EM and DN-L groups to visualize differentially expressed proteins (Figures 2B-2G). In the context of pairwise comparisons between groups, proteins exhibiting differential expression were visually represented as those that showed increased and decreased levels (Figure 2H). A closer look at the two DN groups had more differentially expressed proteins from the NC and DM groups, and that the

- 1 NC group in particular had the most differentially expressed proteins compared to DN-
- 2 EM and DN-L. Then, we selected all differentially expressed proteins from pairwise
- 3 comparisons between groups and plotted UpSet plots of them, which hinted at 40
- 4 common upregulated proteins and 23 common downregulated proteins in DN-EM
- 5 versus NC, DN-L versus NC, DN-EM versus DM and DN-L versus DM (Figures 2I-
- 6 2J; black arrow). The list of 40 common upregulated and 23 downregulated
- 7 differentially expressed proteins was showed in Supplementary Table S1-S2.

8 Serum proteomics revealed the progression of diabetic nephropathy

- 9 With serum proteomics, we performed the fuzzy c-means algorithm ¹⁹ to cluster the
- underlying protein determinants of DN progression and onset in circulation. It can
- cluster the associated protein expression patterns, and proteins in the same cluster
- display similar expressive variation trends. A total of 5 distinct clusters of temporal
- patterns representing different regulated proteins were observed (Figure 3). In these
- clusters, cluster 1 represents downregulated proteins, clusters 2 and 5 represent
- upregulated proteins, and clusters 3 and 4 represent bi-modally expressed proteins. In
- this study, we focused on proteins that are elevated during DN progression. An analysis
- of gene ontology (GO) of proteins in each cluster (Supplementary Figure S1) revealed
- that the upregulated proteins tend to perform a variety of functions, including
- 19 extracellular matrix (ECM) structural constituent, cell adhesion molecule binding,
- 20 ECM, endoplasmic reticulum lumen and biological adhesion (Cluster 2), presumably
- 21 responsible for cell growth, polarity, shape, migration and metabolic activity in DN.
- 22 KEGG pathway enriched proteomics in Cluster 2 are mainly associated with protein
- 23 digestion and absorption, PI3K-Akt signaling pathway, human papillomavirus
- 24 infection, ECM-receptor interaction and protein processing in endoplasmic reticulum
- 25 (Figure 3 and Supplementary Figure S2).
- 26 For reliable DN diagnostic indicators, we set the membership of cluster, the relative
- standard deviation within groups, and the number of unique peptides in cluster 2. A
- 28 total of 16 peptides were eligible and derived from different 15 proteins, including
- 29 ADAMDEC1, ADAMTSL4, AMBP, APOA4, AZGP1, CD44, COL18A1, COL6A3,

- 1 EEA1, FBLN1, FBN1, HMGB1, MAN1A1, OAF and PTPRG (Supplementary Table
- 2 S3). Each peptide's expression levels across all four groups were compared (Figure 4A),
- and the panel of FBLN1, AZGP1, CD44, ADAMDEC1, ADAMTSL4 and HMGB1
- 4 showed significant differences (P < 0.001). To investigate the mechanism of DN
- 5 progression, PPI network data were constructed by inputting 15 proteins into the
- 6 STRING Database, then uploaded into Cytoscape, and selected the top 21 core proteins
- 7 using the Cytohubba plug-in, based on descending degrees (Figure 4B). Based on the
- 8 highest scores, CD44, HMGB1 and AMBP may play a crucial role in DN progression.
- 9 These 15 proteins were also subjected to enrichment analysis for GO and KEGG, whose
- 10 functions are mainly related to ECM structure and receptor interaction, and ECM
- deposition plays an important role in DN development (Figure 4C).
- 12 High mobility group protein B1 is a biomarker for monitoring diabetic
- 13 **nephropathy**
- Analysis of co-expression networks serves as a valuable tool in unraveling the intricate
- changes characteristic of DN. This is particularly essential because the emergence of
- DN phenotypes stems from the amalgamation of numerous and gradual alterations in
- the deregulated expression of multiple proteins, rather than the isolated deregulation of
- individual proteins. ²⁰. Co-expression network analysis was conducted using all
- 19 proteins with the weighted gene co-expression network analysis (WGCNA) approach
- 20 21. Soft thresholding power ($\beta = 8$; cut-off = 0.85) with increased adjacency was used
- 21 to create a weighted gene network (Supplementary Figure S3), resulting in five distinct
- 22 modules of different colors (Figure 5A). Initial visualization of the Topological Overlap
- 23 Matrix (TOM) of proteins after DN was performed using a heatmap plot with various
- 24 module assignments and protein dendrograms (Figure 5B). Based on this, the module-
- 25 trait relationship between the module eigengene E and the trait DN were then
- 26 investigated, the DN group contains all of the proteins from the DM, DN-EM and DN-
- 27 L groups (Figure 5C). Interestingly, only blue module is most significantly correlated
- both with the trait NC (cor = 0.51 and P = 0.01) and DN (cor = 0.45 and P = 0.03).
- 29 Finally, we explored the overlap of proteins in blue module and cluster 2 with a Venn

- diagram (Figure 5D). The overlapping proteins (HMGB1, CD44, FBLN1, PTPRG and
- 2 ADAMTSL4) were display in Table 2 with their relevance scores of DN, which are
- 3 obtained from the Genecards database.
- 4 In our analysis, our research indicates a significant connection between the serum
- 5 protein High mobility group protein B1 (HMGB1) and the development of DN. We
- 6 tested HMGB1's ability to discriminate between patients who developed DN and those
- 7 who did not. Based on ROC curve analysis, we found that HMGB1 was a good marker
- 8 for distinguishing DN-EM versus NC (AUC of ROC = 0.917), DN-L versus NC (AUC
- 9 of ROC = 1.000), DN-EM versus DM (AUC of ROC = 0.889) and DN-L versus DM
- 10 (AUC of ROC = 1.000) (Figure 6A). Furthermore, intensity of HMGB1 was inversely
- related to eGFR (*Pearson*'s R = -0.787 and P < 0.001) and the blood urea nitrogen to
- serum creatinine ratio (*Pearson*'s R = -0.631 and P < 0.001). Meanwhile, intensity of
- HMGB1 was positively correlated blood urea nitrogen (*Pearson*'s R = 0.646 and
- 14 P < 0.001), serum creatinine (*Pearson*'s R = 0.688 and P < 0.001) and cystatin c
- 15 (Pearson's R = 0.661 and P < 0.001) (Figures 6B-6F). These findings suggest that
- 16 HMGB1, particularly when it comes to individuals in the early and advanced stages of
- DN, may accurately monitor the status of the disease.

18

Investigation of high mobility group protein B1 in diabetic nephropathy model

- 19 Although serum proteome profiling method does not require that specific protein
- 20 epitopes be detected, further research is needed to determine if their biological response
- 21 can be applied across species and sources. Injection of streptozotocin (STZ) can
- 22 generate well-established diabetic mouse models, and these can commonly be used to
- 23 study the pathogenesis of DN. We took advantage of a diabetic mice to determine the
- role of HMGB1 on improving the development of DN. Diabetic mice at 28 weeks with
- severe pathophysiologic alterations observed in the kidney compared to diabetic mice
- at 20 weeks. As diabetes progressed, the renal tissues showed increasing damage,
- 27 collagen deposition, and irregular thickening of the basement membrane, indicating
- 28 that the diabetic mouse model was feasible (Figure 7A). Compared to the control group,
- 29 mice injected with STZ at 20 and 28 weeks had significantly higher blood glucose

- levels (Figure 7B), and most importantly, their serum creatinine (Figure 7C), urea nitrogen (Figure 7D) and urinary microalbumin to creatinine ratio (ACR; Figure 7E)
- 3 levels, which reflect the change in kidney function, increased gradually with diabetes.
- 4 HMGB1, a biomarker we identified as being linked to DN in human serum, also
- 5 displayed a noteworthy upregulation as diabetic mice progressed through renal tissues.
- 6 Immunofluorescence (Figure 7F) and Western blot analysis (Figure 7G) revealed that
- 7 the kidney tissues of diabetic mice with renal injury have higher levels of HMGB1, and
- 8 that this level increases with the duration of diabetes. Interestingly, the expression of
- 9 HMGB1 in the kidney tissues of control mice increased with age, although it was not
- statistically significant (Figure 7G). Additionally, an in vitro model of DN renal tubular
- epithelial cells (HK2 cells) was established. A time-dependent culture of HK2 cells in
- 12 high-glucose medium (30 mM) increased HMGB1 protein level at 36 hours as
- epithelial-mesenchymal transition (EMT) changes intensified (Figure 7H). Observing
- treated HK2 cells for HMGB1 expression by immunofluorescence showed increased
- expression of HMGB1 in the nucleus and cytoplasm after high-glucose-stimulated HK2
- cells (Figure 7I). Our data implicate that HMGB1 is a newly identified marker that we
- can evaluate as a potential marker to monitor the progress of DN.

18

19

DISCUSSION

- 20 In this study, comprehensive quantitative proteomics on serum from four independent
- 21 cohorts was conducted to determine biomarkers of DN progression. First, we quantified
- 22 thousands of proteins with discovery mass spectrometry without prior knowledge,
- 23 which allowed us to identify proteins not previously associated with DN. After protein
- 24 relative quantification between NC, DM, DN-EM and DN-L patients the elevated
- 25 expressive variation trend of a total of 15 proteins was further identified in DN
- 26 progression by Mfuzz clustering analysis. We further identified five proteins from
- overlapping analysis between rising cluster 2 and WGCNA, which were measured to
- discriminate between patients who developed DN and those who did not. Based on the

1

results, we explored Genecard's database of DN scores and found that HMGB1 was the

priority biomarker in the development of DN and was tested in both cell and animal 2 models of high glucose. 3 Although proteomics can be utilized in treating many diseases ²², early diagnosis of DN 4 by proteomics has been a challenge ²³. Several studies have shown that profiling urinary 5 proteomics can identify novel biomarkers for DN ^{24,25}. Nevertheless, few trials have 6 been conducted to assess the monitoring value of blood for the course of DN, especially 7 the early diagnosis of DN ^{16,17}. In early DN diagnosis, proteomics may be limited due 8 to vast heterogeneity and widespread protein abundance in blood, as well as strong 9 proteolytic activity, which can muddle interpretation of the blood proteome ²⁶. In our 10 study, we filtered out the high abundance of interfering signals using Field-Asymmetric 11 Ion Mobility Spectrometry (FAIMS), which can selectively identify compounds in a 12 complex background, and detect more key proteins in blood ²⁷. 1602 proteins were 13 identified by filtering out the high abundance of proteins, of which 1402 could be 14 quantified (Figure 1B). Based on the disease course, PCA analysis of 1402 quantified 15 16 proteins and heat map analysis of 484 differentially expressed proteins showed 17 significant protein expression changes in the serum of patients in the DN stage (Figure 1E, 2A), indicating the various molecular alterations induced by DN also affect the 18 expression in serum, especially early stages ²⁸. Although the serum proteome changed 19 20 much less both in NC versus DM and DN-EM versus DN-L, the cohort with early DN had clearer differences than the DM cohort, which facilitated finding biomarkers for 21 22 early DN (Figure 2H). 23 Variations in eGFRs are known to monitor DN progression, but compensatory changes in the remaining nephrons might overestimate or underestimate the true GFR in the 24 condition ²⁹. In the present work, we group 4 cohorts: healthy, diabetic, early medium 25 stage, and late stage of DN, to gain a better understanding of serum protein alterations 26 during DN progression. On the basis of this category, we cluster the associated proteins 27 with similar expressive variation trends in DN progression (Figure 3). In Cluster 2, 28 proteomics has increased along with DN progression, and proteins with high expression 29

are generally more detectable. In KEGG pathway enriched proteomics of Cluster 2 1 2 (Figure 3 and Supplementary Figure S2), one of the most prominent signaling pathways was the PI3K-AKT pathway, consistent with previous studies demonstrating that PI3K-3 AKT signaling is implicated in DN ^{30,31}. Similar to our result, PI3K/Akt signaling 4 contributes to ECM accumulation, which promotes the progression of renal interstitial 5 fibrosis in DM ^{32,33}. To differentiate early DN from DM, we further refined screening 6 biomarkers. Overall, 15 biomarkers strongly associated with DN progression were 7 8 screened in Cluster 2 and mainly related to ECM structure and receptor interaction. In DN progression, ECM proteins are frequently deposited in the mesangium and renal 9 tubule interstices of the glomerulus and basement membranes of patients with DN 34 . 10 Because DN progression involves multiple factors and has a complex proteins 11 12 alteration ³⁵, a comprehensive analysis of multiple deregulated proteins is needed to monitor DN progression ³⁶. Thus, using WGCAN and Mfuzz, we obtain 5 biomarkers 13 (HMGB1, CD44, FBLN1, PTPRG and ADAMTSL4) that were highly correlated with 14 15 DN progression (Figure 5). Among the 5 candidate biomarkers, HMGB1, the most 16 promising biomarker relevant to DN, has been verified in both cell and animal models of high glucose (Figure 7). A nonhistone protein HMGB1 is mainly located inside the 17 nucleus of a cell ³⁷. When the cell is stimulated by various kinds of damage, it releases 18 itself into the extracellular space as a damage-associated molecular pattern (DAMP) 19 molecule that participates in inflammatory responses, differentiation and migration of 20 cells ^{38,39}. HMGB1, as a pathogenic factor in DN, interacts with TLRs and RAGE, 21 which are its receptors on the cytomembrane, activating innate immune responses by 22 promoting nuclear translocation of transcription factors ⁴⁰⁻⁴². Interestingly, high levels 23 of HMGB1 in serum from patients with DN can induce podocyte autophagy, apoptosis, 24 and EMT ⁴³. We speculate that after persistent high glucose stimulation in DN, HMGB1 25 may be released from the nucleus into the extracellular space, triggering positive 26 feedback through TLRs and RAGE receptors that further exacerbates renal fibrotic 27 factors. However, in order to understand the detailed mechanism, further investigation 28 is required. In addition, studies have shown that HMGB1 is elevated both in DN 29

patients' kidney tissues and in those from DN mice, which is consistent with our 1 findings ⁴⁴ (Figure 7G). In addition to the HMGB1 mentioned above, CD44 is a cell 2 adhesion molecule, and its ligands are various ECM components ^{45,46}. CD44 regulates 3 the expression of ECM derived from parietal epithelial cells (PEC) and podocytes in 4 DN ⁴⁷. Another candidate biomarker, FBLN1, is a secreted glycoprotein that interacts 5 with ECM proteins to maintain ECM integrity ⁴⁸. Exosomal FBLN1 promotes DN 6 progression through inducing EMT in the proximal renal tubules ⁴⁹. Patients with CKD 7 and T2DM showed an increased risk of cardiovascular events when their circulating 8 FBLN1 levels were elevated 50. The remaining two biomarkers, PTPRG and 9 ADAMTSL4, have not been associated with DN, similar to what we found in our results. 10 Nevertheless, to determine whether these proteins are diagnostic biomarkers for DN 11 progression, additional large-scale investigations are needed. 12 Our research showed that HMGB1 was highly correlated with several renal function 13 indicators (Figures 6B-6F) and could be a good marker for the early detection of DN, 14 especially distinguishing healthy control and DN patients (Figure 6A). Based on our 15 results, HMGB1 may be identified as a potential novel biomarker for DN progression. 16 17 Of course, as a single biomarker, HMGB1 also has limitations. As the age confounder factor could not be excluded in DN patients (Table S4; β =8552.354, P=0.011), the 18 expression of HMGB1 in the kidney tissues of control mice increased with age, which 19 20 hinted that the elevation of HMGB1 may be related to age factors (Figure 7G). Furthermore, HMGB1 proteins could serve as a potential non-invasive biomarker for 21 several inflammation-related diseases or tumors⁵¹⁻⁵³. Inflammation is also crucial to DN 22 progression⁵⁴, which seems that HMGB1 might serve as a general biomarker of early 23 inflammation. By combining other biomarkers, the monitoring accuracy of HMGB1 in 24 DN progression might improve. Intriguingly, a candidate biomarker in our study is 25 CD44, which is increased by extracellular HMGB1 in tumor progression⁵⁵. However, 26 it's not clarified whether HMGB1 and CD44 can be combined to monitor DN 27 progression, and whether HMGB1 increases CD44 to regulate it. Thus, further clinical 28

- sample prediction models and mechanism studies are urgently needed to clarify the role
- 2 of HMGB1 as a potential biomarker for early DN progression.
- 3 A novel aspect of this study is that, based on the stages of DN patients and clustering
- 4 analyses of proteins with similar altered trends in progression, we were able to identify
- 5 biomarkers in serum that can reflect DN progression more accurately. A validated
- 6 biological response of HMGB1 was found across species and sources, making it a
- 7 reliable biomarker for DN progression, but clinical translation needs more exploration.
- 8 In conclusion, we investigated the proteomes of patients with DM or different stages of
- 9 DN and healthy control by quantitative proteomics to gain an understanding of serum
- protein alterations during DN progression. Five promising biomarkers, HMGB1, CD44,
- 11 FBLN1, PTPRG and ADAMTSL4, allowed monitoring of the progression of DN,
- whereas HMGB1 was highly correlated with renal function alterations and could be an
- appropriate marker for the early detection of DN, especially distinguishing healthy
- controls and DN patients. Although there is insufficient evidence to conclude that these
- biomarkers can replace invasive diagnostics for DN, with further research, these
- proteomics changes may help clinicians identify DN in the early stages.

17

18

LIMITATIONS OF THE STUDY

- 19 Despite our findings, this study has several limitations. First, as this study only involves
- a small number of patients, it is necessary to validate the results with additional patients
- 21 within each cohort. Statistics show significant differences in all results, and with
- increased sample size, the difference in HMGB1 elevation in serum of DN patients may
- 23 increase. Second, there were not enough clinical data collected in this retrospective
- study, so no adjustments for clinical covariates or pathological confounders were made.
- 25 Third, the HMGB1 is an inflammation-associated molecule, and many
- 26 proinflammatory factors must be considered before it can be used as a biomarker for
- 27 DN. Thus, more research cohorts with DN are needed to validate the biomarker. Fourth,
- 28 the findings from our study were limited to a single hospital, which may limit their

- 1 generalizability. Finally, non-diabetic chronic kidney disease was not profiled for
- 2 serum proteomics, so we cannot infer that the serum protein alterations in DN are
- 3 exclusively due to diabetes.

4

5 **ACKNOWLEDGMENTS**

- 6 This study was funded by grants from the National Natural Science Foundation of
- 7 China (81860134), the Guizhou Provincial Natural Science Foundation (ZK [2023] 377)
- and the Guizhou Provincial Natural Science Foundation (ZK [2023] 379).

9

10 **AUTHOR CONTRIBUTIONS**

- 11 Conceptualization: LL. Writing original draft: RP. Methodology: RP and SZ.
- Software: RP and SZ. Formal analysis: RP. Visualization: RP. Writing review &
- editing: SZ, XL and LL. Funding acquisition: LL, XL and QZ. Sample collection: YH.
- Data collection: XL and YH. Construct animal model: SC, XZ and HL. Cell model
- experiments: MC, YY and HY. Supervision: LL and BG. Project administration: LL
- and BG.

17

18

DECLARATIONS OF COMPETING INTEREST

19 The authors declare no competing interests.

20

1 Figure legends

- 2 Figure 1. Design and quality control of serum proteomics in DN.
- 3 (A) Overview of the study structure and cohort particulars: In total, 96 participants from
- 4 healthy control, diabetic, and diabetic nephropathy were recruited and further divided
- 5 into four groups, including healthy control (NC), diabetic (DM), early medium stage
- 6 (DN-EM), and late stage (DN-L), with 6 patients in each group to perform liquid
- 7 chromatography-tandem mass spectrometry (LC-MS/MS) analysis.
- 8 (B) Overview of the number of proteins identified by LC-MS/MS analysis.
- 9 (C) Distribution of identifiable peptide lengths from LC-MS/MS analysis.
- 10 (D) Pearson's Correlation Coefficient (PCC) analysis from the proteomics data in NC,
- DM, DN-EM, and DN-L groups. Color saturation in red and blue indicates a degree of
- correlation present among the samples.
- 13 (E) Principal component analysis (PCA) from the proteomics data shows
- discrimination between NC (gray), DM (yellow), DN-EM (blue), and DN-L (red)
- groups. Each dot represents a single sample.
- 16 (F) Relative Standard Deviation (RSD) from the proteomics data shows intra-group
- data repeatability in NC (gray), DM (yellow), DN-EM (blue), and DN-L (red) groups.

18 Figure 2. Serum proteome profiling of patients with DN

- 19 (A) Heatmap of differential expressed proteins (DEPs) from the proteomics data in NC,
- 20 DM, DN-EM, and DN-L groups. Red: upregulated proteins; blue: downregulated
- 21 proteins.
- 22 (B-G) Volcano plots of DEPs from the proteomics data for each pairwise comparison
- 23 (P < 0.05, FC > 1.5 and FC < 1/1.5). Gray: proteins that are not significantly deregulated;
- red: upregulated proteins; blue: downregulated proteins.
- 25 (H) Overview of the increased and decreased DEPs from the proteomics data for each
- 26 pairwise comparison. Red: upregulated proteins; blue: downregulated proteins.

- 1 (I-J) UpSet plots show the intersections between DEPs from the proteomics data for
- 2 each pairwise comparison (red sets, upregulated proteins; blue sets, downregulated
- 3 proteins). Circles connected to the intersection indicate which DEPs are included in the
- 4 intersection, and the size of the intersection is displayed in the main bar (right bars).

5 Figure 3. Mufzz analysis reveals different expression patterns of proteins in DN

6 **Progression**

- 7 A protein expression line graph is shown on the left, a heat map is shown in the middle,
- 8 and the top 2 enrichment analysis entries are shown on the right. Line graph: the
- 9 horizontal axis represents the sample, the vertical axis depicts the relative protein
- expression, a line represents a protein, and the color of the line indicates the affiliation
- intensity in the cluster. Heatmap: the horizontal axis represents the sample, the vertical
- 12 axis depicts different proteins, and the heatmap color indicates the relative expression
- of the protein in the sample. Domain enrichment is red, Gene Ontology Biological
- Process (GO-BP) enrichment is blue, Gene Ontology Cellular Component (GO-CC)
- enrichment is green, Gene Ontology Molecular Function (GO-MF) enrichment is
- purple, and Kyoto Encyclopedia of Genes and Genomes (KEGG) enrichment is orange.

17 Figure 4. A panel of proteins strongly associated with DN progression

- 18 (A) Box-and-whisker plot to visually represent the dispersion of LFQ intensity values
- 19 for APOA4, FBLN1, OAF, MAN1A1, AZGP1, EEA1, PTPRG, FBN1, CD44,
- 20 ADAMDEC1, ADAMTSL4, COL18A1, COL6A3, AMBP and HMGB1 in serum. NC
- 21 is gray, DM is yellow, DN-EM is blue, DN-L is red. A median line is shown in the
- 22 middle of the box, the top and bottom represent the upper and lower quartiles, and
- 23 whiskers indicate the upper and lower limits for outliers. *P < 0.05, **P < 0.01, ***P
- < 0.001, ****P < 0.0001 by multiple comparison.
- 25 (B) PPI network showing the interactions of the 15 proteins (shown in Figure 4A) based
- on STRING. The darker the node, the more core the interaction.
- 27 (C) Gene enrichment analysis (BP: GO-BP, CC: GO-CC, MM: GO-MF, KEGG) of 15
- 28 proteins (shown in Figure 4A). The horizontal axis represents the ratio of proteins, the

- 1 vertical axis represents enrichment analysis entries, the color shades represent adjust P-
- 2 values, and the circle size represents the protein number.

3 Figure 5. Novel biomarkers associated with DN progression achieved by WGCNA

- 4 (A) Cluster dendrogram of the topological overlap between proteins. Highly similar
- 5 modules are delineated by hierarchical clustering dendrograms and assigned arbitrary
- 6 colors to each module below.
- 7 (B) The dendrogram and network heatmap plot of the topological overlap between
- 8 proteins. A module membership, color-coded for easy identification, is displayed below
- 9 and to the right of the dendrograms. The color saturation in yellow and red indicates a
- greater degree of interconnection between co-expressions.
- 11 (C) Heatmap of the module-trait relationship between the module eigengene E and the
- trait DN. An eigengene corresponds to each row, and a trait to each column.
- 13 (D) Venn diagram of DEPs in the blue module and 15 proteins (shown in Figure 4A)
- 14 from cluster 2.

15 Figure 6. The diagnosis values of HMGB1 in DN progression

- 16 (A) Receiver-operating characteristic (ROC) curve of HMGB1 for each pairwise
- 17 comparison. AUC, area under the ROC curve. AUC has low diagnostic accuracy at 0.5
- to 0.7, certain diagnostic accuracy at 0.7 to 0.9, and high diagnostic accuracy at 0.9 or
- 19 more.
- 20 (B-F) Pearson correlation between intensity of HMGB1 and eGFR, blood urea nitrogen
- 21 to serum creatinine ratio (BUN/Scr), blood urea nitrogen, serum creatinine, and cystatin
- c, respectively. R > 0 represents positively correlated, and R < 0 represents inversely
- 23 correlated.

24

Figure 7. Validation of HMGB1 in DN model

- 25 (A) Hematoxylin and eosin staining (HE), masson trichrome staining, and periodic
- 26 acid-schiff staining (PAS) staining show typical DN changes in diabetic mice; scale

- 1 bars = 50 μm; inflammatory cell infiltration (yellow arrow), collagen deposition (black
- 2 arrow), and irregular thickening of the glomerular basement membrane (red arrow) and
- 3 glomerular capsule (green arrow). NC20W and NC28W is normal mice at 20 and 28
- 4 weeks, DM20W and DM28W is diabetic mice at 20 and 28 weeks.
- 5 (B-E) Blood glucose, serum creatinine, and blood urea nitrogen levels and urine
- 6 albumin to creatinine ratio of normal mice (blue) and diabetic mice (red).
- 7 (F) Immunofluorescence staining for HMGB1 (red) and lotus tetragonolobus lectin
- 8 (LTL, green, the marker of renal tubular brush brush) in the kidney tissues of mice;
- 9 scale bars = $50 \mu m$.
- 10 (G) In the analysis of kidney tissue from mice, Western blotting was utilized to ascertain
- the expression levels of HMGB1 as well as proteins associated with epithelial-
- mesenchymal transition (EMT); quantification of relative levels of protein expression.
- 13 (H) Western blotting was employed to assess the expression of HMGB1 and proteins
- indicative of EMT in HK2 cells stimulated with high glucose.
- 15 (I) Immunofluorescence staining for β-actin (red) and HMGB1 (green) in high-glucose-
- stimulated HK2 cells; white arrow is cytoplasm; scale bars = $20 \mu m$.
- All experiments are performed three times and data were expressed as mean \pm standard
- deviation (SD). *P<0.05, **P<0.01 and ***P<0.001 by Student's t-test.

19

1	STA	R	M	FT	HC	DS
1	OIB		IVI	Ľ	111	טענ

2 KEY RESOURCES TABLE

3 RESOURCE AVAILABILITY

4 Lead contact

- 5 For additional details and inquiries regarding resources and reagents, please contact the
- 6 primary point of contact, Lirong Liu (Email: lirongliu@gmc.edu.cn).

7 Materials availability

8 In this study, no novel reagents were developed.

9 Data and code availability

- 10 **1** The mass spectrometry proteomics data have been deposited to the
- ProteomeXchange Consortium via the PRIDE ⁵⁶ partner repository with the dataset
- identifier PXD047872.
- 13 This paper does not report original code.
- 14 Any additional information required to reanalyze the data reported in this paper is
- available from the lead contact upon request.

16

17

18

EXPERIMENTAL MODEL AND STUDY PARTICIPANT DETAILS

Clinical Samples

- 19 The study population was all Han Chinese, comprising healthy control (NC, n=33,
- 20 54.67±18.24 years, male: 10, female: 23), diabetic (DM, n=34, 57.03±16.07 years, male:
- 21 20, female: 14), and diabetic nephropathy (DN, n=29, 62.10±10.69 years, male: 16,
- female: 13) patients enrolled from July 2021 to January 2022 at the Affiliated Hospital
- of Guizhou Medical University. In accordance with the Declaration of Helsinki 1975,
- 24 this study was approved by the Ethics Committees of the Affiliated Hospital of Guizhou

- 1 Medical University (Ethics Approval No.2023398). Consent forms have been signed
- 2 by all participants for the extra samples to be used for academic research.

3 Inclusion and Exclusion criteria

- 4 Inclusion criteria include (1) all patients except the NC group fulfilling the diagnostic
- 5 criteria of DM; (2) for NC and DM group, eGFR ≥ 90 ml/min/1.73 m² without kidney
- 6 disease; (3) for DN group, with kidney disease and diabetic retinopathy, eGFR less than
- 7 90 ml/min/1.73 m².
- 8 Exclusion criteria include (1) other urinary diseases as hereditary kidney disease,
- 9 urinary tract infection, stones or obstruction; (2) systemic diseases, atherosclerosis,
- severe hypertension, thrombotic microangiopathy, active or chronic infectious diseases;
- 11 (3) complication of serious diseases as well as a tumor; (4) pregnant woman.

12 Animals and procedures

- We sourced male C57BL/6 mice (6–8 weeks old) bred under specific pathogen-free
- 14 (SPF) conditions from Charles River Co. Ltd (Beijing, China). All mice were randomly
- grouped (n=3), and DM mice were injected with STZ (Solarbio, S8050) through the
- intraperitoneal at a dose of 55 mg/kg/day, while NC mice received solvent injections
- of the same volume. Experiments were conducted on mice with random blood glucose
- \geq 16.7 mmol/L and positive urine glucose. At 20 and 28 weeks, mice were killed, then
- kidney tissues, blood and urine were collected. All animal experiments were approved
- 20 by China's National Health and Medical Research Council's Code for the Care (No.
- 21 1800353).

22

Cell culture

- 23 Human renal proximal tubule epithelial cells (HK2) were cultured in Dulbecco's
- 24 modified Eagle's/F12 medium (DMEM/F12, 1:1) under standard conditions of 37°C
- and 5% CO2. All mediums were supplemented with 10% fetal bovine serum (Gibco-
- 26 BRL) and 1% penicillin/streptomycin. HK2 cells were cultured with 30 mM D-glucose
- 27 (HG; Solarbio, G8150) mediums at different time point⁵⁷.

METHOD DETAILS

1

2

28

Sample collection and proteomics assays

3 Serum samples from fasting blood were collected by centrifugation at 3500 rpm for 10 min at room temperature and stored at -80 °C until assayed. The cell debris was 4 removed by centrifuged at 12000 g for 10 min at 4 °C, then depleted of high-abundance 5 proteins using the PierceTM Top 12 Abundant Protein Depletion Spin Columns Kit 6 7 (Thermo Fisher Scientific, 85164) according to the manufacturer's instructions. Protein concentration was determined using BCA kit (Beyotime, P0011). 8 An equivalent quantity of protein was utilized for enzymatic hydrolysis in every sample. 9 The volume was standardized, and subsequently, dithiothreitol (DTT) was introduced 10 to achieve a final concentration of 5 mM. This mixture was then subjected to reduction 11 at 56°C for a duration of 30 minutes. Subsequent to that, iodoacetamide (IAA) was 12 incorporated to attain a final concentration of 11 mM. This concoction was left to 13 incubate in darkness for a duration of 15 minutes at room temperature. Afterward, the 14 15 samples were carefully transferred into ultrafiltration tubes and subjected to centrifugation at 12000 g for a span of 20 minutes, all at room temperature. Following 16 this centrifugation step, the samples underwent a thorough washing process, involving 17 three successive washes with 8M urea, followed by an additional three rounds of 18 washing with the replacement buffer. In the final step, trypsin was incorporated at a 19 proportion of 1:50 (trypsin to protein, m/m) to facilitate an overnight digestion process. 20 Following centrifugation at 12000 g for a duration of 10 minutes at room temperature 21 22 to recover the peptides, they were also recovered using ultrapure water once and then 23 mixed together. For the examination of serum samples, a liquid chromatography-tandem mass 24 spectrometry (LC-MS/MS) approach was employed. This involved utilizing an 25 Orbitrap ExplorisTM 480 mass spectrometer (Thermo Fisher Scientific) in tandem with 26 27 an EASY-nLC 1200 Ultra high-performance liquid phase system (UHPLC, Thermo

Fisher Scientific). The mass spectrometry was used to analyze the ionized peptides after

they had been separated by the UHPLC and introduced into the NSI ion source for 1 ionization. Mass spectrometry was set for primary scan range of 400-1200 m/z, at 2 60000 resolution; secondary scan range of 100 m/z, at 30000 resolution, without 3 TurboTMT. Data-dependent scanning (DDA) software was utilized in the data 4 collecting mode. Automatic gain control (AGC) was set to 75% to maximize the 5 6 effective use of the mass spectrum. The signal threshold was defined at 1E4 ions/s, with a maximum injection time of 100ms. Additionally, a dynamic exclusion time of 30s 7 8 was applied to tandem mass spectrometry scans to ensure avoidance of duplicate scanning for parent ions. The service of proteomics assays was provided by PTM 9 10 Biolabs, Inc.

Proteomics Data Analysis

11

19

Each protein was subjected to a two-sample t-test for each pairwise comparison across 12 the four groups. Absolute \log^2 (fold change) > 1.5 or < 1/1.5 and a *P*-value < 0.05 were 13 used to designate differentially expressed (DE) proteins. Following log2 ratio 14 15 transformation, the relative protein expression was screened by a standard deviation (SD) > 0.3. The 828 proteins remained, and Mfuzz clustering analysis was used to 16 separate proteins in the same cluster with similar expression trends into five clusters. 17 The most relevant peptides from the cluster 2 group (n = 16) were selected after setting 18 unique peptides ≥ 2 , membership of cluster $2 \geq 0.4$, relative standard deviation (RSD) \leq 0.4, and a P-value < 0.05 among samples. The examination of the protein-protein 20 interaction (PPI) network involved the utilization of the Search Tool for the Retrieval 21 22 of Interacting Genes (STRING; http://string-db.org). Cytoscape software (version 3.9.1) 23 was used to construct a PPI network from an interaction with a combined score of more than 0.4. Gene Ontology (GO), Kyoto Encyclopedia of Genes and Genomes (KEGG) 24 enrichment analysis and Weighted Gene Co-Expression Network Analysis (WGCNA) 25 were performed using R software (version 4.2.1). For WGCNA, soft thresholding 26 power ($\beta = 8$; cut-off = 0.85) was chosen to increase the adjacency matrix, which was 27 converted into a topological overlap matrix. The minModuleSize was set to 50 to 28 hierarchically cluster the modules, and then DN related modules were merged. The 29

- 1 relevance scores of DN were searched from the Genecards database
- 2 (https://www.genecards.org/).

3 Receiver operating characteristic (ROC) and correlation analysis

- 4 The diagnostic sensitivity and specificity of HMGB1, along with the correlation
- 5 between HMGB1 and clinical diagnostic indicators, were examined using R software
- 6 (version 4.2.1). With R packages "pROC", receiver operator characteristic curves were
- 7 plotted for HMGB1 in DN and the area under the curve (AUC) estimated. AUC ranging
- 8 from 0.7 to 0.9 signified a well-fitted model, while an AUC exceeding 0.9 indicated a
- 9 highly fitting model.

Immunoblotting

10

- Renal tissues were homogenised and sonicated using RIPA lysis buffer, supplemented
- with 1mM phenylmethanesulfonyl fluoride (PMSF, Solarbio, P0100). Additionally,
- cells were lysed using RIPA lysis buffer (1mM PMSF). After protein extraction, the
- separation process was carried out on SDS-PAGE gels. Subsequently, these proteins
- were transferred onto polyvinylidene difluoride (PVDF) membranes (Millipore,
- 16 ISEQ00010). After a 1 hour blocking step at room temperature using 5% (w/v) nonfat
- milk, the membrane underwent an overnight incubation at 4 °C with antibodies against
- 18 E-cadherin (Proteintech, 20874-1-AP), Vimentin (Proteintech, 10366-1-AP), β-actin
- 19 (Proteintech, 66009-1-Ig), and HMGB1 (Abcam, ab79823). This was followed by a
- 20 subsequent 1 hour incubation at room temperature with secondary antibodies (CST,
- 21 7074 and 7076;). Enhanced chemiluminescence reagents (Absin, abs920) and ImageJ
- 22 (National Institutes of Health, V1.8.0) were used to visualize and analyze the protein
- 23 bands.

24

Histology analysis

- 25 For histological observation of renal morphology, the renal tissues were fixed in 4%
- buffered paraformaldehyde, embedded in paraffin, and sliced at 3 millimeters. In
- accordance with the protocol, hematoxylin and eosin staining (HE; Solarbio, G1220),
- 28 Masson trichrome staining (Solarbio, G1346), and periodic acid-schiff staining (PAS;

- Solarbio, G1281) were performed, and the stained sections were analyzed using a
- 2 computational color image analysis system (Leica Microscope, Germany DM2500).
- 3 Utilizing ImageJ software, the collagen tissue area was calculated to assess renal
- 4 fibrosis quantitatively.

5 **Biochemical assays**

- 6 Blood and urine were measured by automatic clinical chemistry analyzer
- 7 (ARCHITECT, c16000).

8 Immunofluorescent staining

- 9 The renal tissues section for immunofluorescent staining was treated in the same
- manner as for histology analysis, and heat-mediated antigen retrieval with Tris/EDTA
- buffer pH 9.0 was carried out before staining was conducted. After fixing with 4%
- buffered paraformaldehyde, 0.3% Triton X-100 was used to permeabilize the HK2 cells.
- 13 Rabbit anti-HMGB1 antibody (Abcam, ab79823); Mouse anti-β-actin antibody
- 14 (Proteintech, 66009-1-Ig) and Lotus Tetragonolobus Lectin (LTL, Biotinylated; Vector
- Laboratories, B-1325-2) were used for immunofluorescence staining, and images were
- obtained under a positive fluorescence microscope (ZEISS, Axio Imager) and a
- 17 confocal microscopy (ZEISS, LMS 710).

18

QUANTIFICATION AND STATISTICAL ANALYSIS

- 19 Statistical analyses of clinical parameters were exclusively conducted using SPSS 26.0
- 20 software. With GraphPad Prism 9.4, 16 candidate peptides and all verification
- 21 experiments were analyzed statistically. R software (version 4.2.1) was used to analyze
- of all proteomics data analysis. A Shapiro-Wilk test was performed on the numerical
- variables of this study for the purpose of testing normality. To compare normal
- variables (mean \pm SD), we used an analysis of variance (ANOVA), while to compare
- variables with non-normality (median, interquartile range), we used the Kruskal-Wallis
- 26 test. Using Fisher's exact test, this study tested classification variables. The factors that
- 27 influenced the rise of HMGB1 were determined using multiple stepwise regressions.

- 1 All statistical tests of verification experiments were performed by the two-tailed
- Student's *t*-test. *P*-value ≤ 0.05 was defined statistically significant.

3

1 References

- 2 1. Cho, N.H., Shaw, J.E., Karuranga, S., Huang, Y., da Rocha Fernandes, J.D., Ohlrogge, A.W.,
- 3 and Malanda, B. (2018). IDF Diabetes Atlas: Global estimates of diabetes prevalence for
- 4 2017 and projections for 2045. Diabetes Res Clin Pract 138, 271-281.
- 5 10.1016/j.diabres.2018.02.023.
- 6 2. Afkarian, M., Zelnick, L.R., Hall, Y.N., Heagerty, P.J., Tuttle, K., Weiss, N.S., and de Boer, I.H.
- 7 (2016). Clinical Manifestations of Kidney Disease Among US Adults With Diabetes, 1988-
- 8 2014. Jama *316*, 602-610. 10.1001/jama.2016.10924.
- 9 3. Fu, H., Liu, S., Bastacky, S.I., Wang, X., Tian, X.J., and Zhou, D. (2019). Diabetic kidney
- diseases revisited: A new perspective for a new era. Mol Metab 30, 250-263.
- 11 10.1016/j.molmet.2019.10.005.
- 4. Gonzalez Suarez, M.L., Thomas, D.B., Barisoni, L., and Fornoni, A. (2013). Diabetic
- nephropathy: Is it time yet for routine kidney biopsy? World J Diabetes 4, 245-255.
- 14 10.4239/wjd.v4.i6.245.
- 15 5. Califf, R.M. (2018). Biomarker definitions and their applications. Exp Biol Med (Maywood)
- *243*, 213-221. 10.1177/1535370217750088.
- 17 6. Group, F.-N.B.W. (2016). In BEST (Biomarkers, EndpointS, and other Tools) Resource,
- 18 (Food and Drug Administration (US) National Institutes of Health (US)).
- 7. Satirapoj, B., and Adler, S.G. (2014). Comprehensive approach to diabetic nephropathy.
- 20 Kidney Res Clin Pract *33*, 121-131. 10.1016/j.krcp.2014.08.001.
- 21 8. Satirapoj, B., and Adler, S.G. (2015). Prevalence and Management of Diabetic
- 22 Nephropathy in Western Countries. Kidney Dis (Basel) 1, 61-70. 10.1159/000382028.
- 23 9. Parving, H.H., Oxenboll, B., Svendsen, P.A., Christiansen, J.S., and Andersen, A.R. (1982).
- 24 Early detection of patients at risk of developing diabetic nephropathy. A longitudinal study
- 25 of urinary albumin excretion. Acta Endocrinol (Copenh) 100, 550-555.
- 26 10.1530/acta.0.1000550.
- 27 10. Fioretto, P., Steffes, M.W., and Mauer, M. (1994). Glomerular structure in nonproteinuric
- 28 IDDM patients with various levels of albuminuria. Diabetes 43, 1358-1364.
- 29 10.2337/diab.43.11.1358.
- 30 11. Barutta, F., Bellini, S., Canepa, S., Durazzo, M., and Gruden, G. (2021). Novel biomarkers of
- diabetic kidney disease: current status and potential clinical application. Acta Diabetol 58,
- 32 819-830. 10.1007/s00592-020-01656-9.
- 33 12. Niu, L., Geyer, P.E., Wewer Albrechtsen, N.J., Gluud, L.L., Santos, A., Doll, S., Treit, P.V.,
- Holst, J.J., Knop, F.K., Vilsboll, T., et al. (2019). Plasma proteome profiling discovers novel
- proteins associated with non-alcoholic fatty liver disease. Mol Syst Biol 15, e8793.
- 36 10.15252/msb.20188793.
- 37 13. Liu, Y., Buil, A., Collins, B.C., Gillet, L.C., Blum, L.C., Cheng, L.Y., Vitek, O., Mouritsen, J.,
- 38 Lachance, G., Spector, T.D., et al. (2015). Quantitative variability of 342 plasma proteins in
- 39 a human twin population. Mol Syst Biol *11*, 786. 10.15252/msb.20145728.
- 40 14. Campion, C.G., Sanchez-Ferras, O., and Batchu, S.N. (2017). Potential Role of Serum and
- 41 Urinary Biomarkers in Diagnosis and Prognosis of Diabetic Nephropathy. Can J Kidney
- 42 Health Dis 4, 2054358117705371. 10.1177/2054358117705371.
- 43 15. Thippakorn, C., Schaduangrat, N., and Nantasenamat, C. (2018). Proteomic and

- bioinformatic discovery of biomarkers for diabetic nephropathy. Excli j *17*, 312-330. 2 10.17179/excli2018-1150.
- 3 16. Colombo, M., Valo, E., McGurnaghan, S.J., Sandholm, N., Blackbourn, L.A.K., Dalton, R.N.,
- Dunger, D., Groop, P.H., McKeigue, P.M., Forsblom, C., and Colhoun, H.M. (2019).
- Biomarker panels associated with progression of renal disease in type 1 diabetes.

 Diabetologia *62*, 1616-1627. 10.1007/s00125-019-4915-0.
- 7 17. Liu, S., Gui, Y., Wang, M.S., Zhang, L., Xu, T., Pan, Y., Zhang, K., Yu, Y., Xiao, L., Qiao, Y., et al. (2021). Serum integrative omics reveals the landscape of human diabetic kidney
- 9 disease. Mol Metab *54*, 101367. 10.1016/j.molmet.2021.101367.
- 10 18. KDIGO 2020 Clinical Practice Guideline for Diabetes Management in Chronic Kidney 11 Disease. (2020). Kidney Int *98*, S1-s115. 10.1016/j.kint.2020.06.019.
- 19. Futschik, M.E., and Carlisle, B. (2005). Noise-robust soft clustering of gene expression time-course data. J Bioinform Comput Biol *3*, 965-988. 10.1142/s0219720005001375.
- Gaiteri, C., Ding, Y., French, B., Tseng, G.C., and Sibille, E. (2014). Beyond modules and hubs: the potential of gene coexpression networks for investigating molecular mechanisms of complex brain disorders. Genes Brain Behav *13*, 13-24.
- 17 10.1111/gbb.12106.
- Langfelder, P., and Horvath, S. (2008). WGCNA: an R package for weighted correlation network analysis. BMC Bioinformatics *9*, 559. 10.1186/1471-2105-9-559.
- 20 22. Dubin, R.F., and Rhee, E.P. (2020). Proteomics and Metabolomics in Kidney Disease, including Insights into Etiology, Treatment, and Prevention. Clin J Am Soc Nephrol *15*, 404-411. 10.2215/cjn.07420619.
- 23. Tofte, N., Persson, F., and Rossing, P. (2020). Omics research in diabetic kidney disease: 24 new biomarker dimensions and new understandings? J Nephrol *33*, 931-948. 25 10.1007/s40620-020-00759-4.
- 26 24. Tofte, N., Lindhardt, M., Adamova, K., Bakker, S.J.L., Beige, J., Beulens, J.W.J., Birkenfeld, A.L., Currie, G., Delles, C., Dimos, I., et al. (2020). Early detection of diabetic kidney disease by urinary proteomics and subsequent intervention with spironolactone to delay progression (PRIORITY): a prospective observational study and embedded randomised placebo-controlled trial. Lancet Diabetes Endocrinol 8, 301-312. 10.1016/s2213-8587(20)30026-7.
- 32 25. Guillén-Gómez, E., Bardají-de-Quixano, B., Ferrer, S., Brotons, C., Knepper, M.A., Carrascal,
 33 M., Abian, J., Mas, J.M., Calero, F., Ballarín, J.A., and Fernández-Llama, P. (2018). Urinary
 34 Proteome Analysis Identified Neprilysin and VCAM as Proteins Involved in Diabetic
 35 Nephropathy. J Diabetes Res 2018, 6165303. 10.1155/2018/6165303.
- 36 26. Kolch, W., Neusüss, C., Pelzing, M., and Mischak, H. (2005). Capillary electrophoresis-mass 37 spectrometry as a powerful tool in clinical diagnosis and biomarker discovery. Mass 38 Spectrom Rev *24*, 959-977. 10.1002/mas.20051.
- Covington, J.A., van der Schee, M.P., Edge, A.S., Boyle, B., Savage, R.S., and Arasaradnam,
 R.P. (2015). The application of FAIMS gas analysis in medical diagnostics. Analyst *140*,
 6775-6781. 10.1039/c5an00868a.
- Swaminathan, S.M., Rao, I.R., Shenoy, S.V., Prabhu, A.R., Mohan, P.B., Rangaswamy, D., Bhojaraja, M.V., Nagri, S.K., and Nagaraju, S.P. (2023). Novel biomarkers for prognosticating diabetic kidney disease progression. Int Urol Nephrol *55*, 913-928.

- 1 10.1007/s11255-022-03354-7.
- 2 29. Colhoun, H.M., and Marcovecchio, M.L. (2018). Biomarkers of diabetic kidney disease.
- 3 Diabetologia *61*, 996-1011. 10.1007/s00125-018-4567-5.
- 4 30. Dong, R., Zhang, X., Liu, Y., Zhao, T., Sun, Z., Liu, P., Xiang, Q., Xiong, J., Du, X., Yang, X., et
- al. (2023). Rutin alleviates EndMT by restoring autophagy through inhibiting HDAC1 via
- 6 PI3K/AKT/mTOR pathway in diabetic kidney disease. Phytomedicine *112*, 154700.
- 7 10.1016/j.phymed.2023.154700.
- 8 31. Wang, X., Jiang, L., Liu, X.Q., Huang, Y.B., Wang, A.L., Zeng, H.X., Gao, L., Zhu, Q.J., Xia, L.L.,
- 9 and Wu, Y.G. (2022). Paeoniflorin binds to VEGFR2 to restore autophagy and inhibit
- apoptosis for podocyte protection in diabetic kidney disease through PI3K-AKT signaling
- 11 pathway. Phytomedicine *106*, 154400. 10.1016/j.phymed.2022.154400.
- 12 32. Zhang, Y., Jin, D., Kang, X., Zhou, R., Sun, Y., Lian, F., and Tong, X. (2021). Signaling
- Pathways Involved in Diabetic Renal Fibrosis. Front Cell Dev Biol *9*, 696542.
- 14 10.3389/fcell.2021.696542.
- 15 33. Li, F., Li, L., Hao, J., Liu, S., and Duan, H. (2017). Src Homology 2 Domain-Containing
- 16 Inositol 5'-Phosphatase Ameliorates High Glucose-Induced Extracellular Matrix
- Deposition via the Phosphatidylinositol 3-Kinase/Protein Kinase B Pathway in Renal
- Tubular Epithelial Cells. J Cell Biochem *118*, 2271-2284. 10.1002/jcb.25881.
- Tuleta, I., and Frangogiannis, N.G. (2021). Diabetic fibrosis. Biochim Biophys Acta Mol Basis Dis *1867*, 166044. 10.1016/j.bbadis.2020.166044.
- 21 35. Tuttle, K.R., Agarwal, R., Alpers, C.E., Bakris, G.L., Brosius, F.C., Kolkhof, P., and Uribarri, J.
- 22 (2022). Molecular mechanisms and therapeutic targets for diabetic kidney disease. Kidney
- 23 Int *102*, 248-260. 10.1016/j.kint.2022.05.012.
- 24 36. Chen, J., Luo, S.F., Yuan, X., Wang, M., Yu, H.J., Zhang, Z., and Yang, Y.Y. (2022). Diabetic
- 25 kidney disease-predisposing proinflammatory and profibrotic genes identified by
- weighted gene co-expression network analysis (WGCNA). J Cell Biochem 123, 481-492.
- 27 10.1002/jcb.30195.
- 28 37. Amato, J., Cerofolini, L., Brancaccio, D., Giuntini, S., Iaccarino, N., Zizza, P., Iachettini, S.,
- 29 Biroccio, A., Novellino, E., Rosato, A., et al. (2019). Insights into telomeric G-quadruplex
- 30 DNA recognition by HMGB1 protein. Nucleic Acids Res 47, 9950-9966.
- 31 10.1093/nar/gkz727.
- 32 38. Niu, Z., Lin, J., Hao, C., Xu, X., Wang, C., Dai, K., Deng, X., Deng, M., Guo, Y., and Yao, W.
- 33 (2022). Glycyrrhizic Acid Attenuates Pulmonary Fibrosis of Silicosis by Inhibiting the
- 34 Interaction between HMGB1 and BRG1 through Pl3K/Akt/mTOR Pathway. Int J Environ
- 35 Res Public Health *19*. 10.3390/ijerph19148743.
- 36 39. Czura, C.J., Wang, H., and Tracey, K.J. (2001). Dual roles for HMGB1: DNA binding and
- 37 cytokine. J Endotoxin Res 7, 315-321. 10.1177/09680519010070041401.
- 38 40. Chen, X., Ma, J., Kwan, T., Stribos, E.G.D., Messchendorp, A.L., Loh, Y.W., Wang, X., Paul,
- 39 M., Cunningham, E.C., Habib, M., et al. (2018). Blockade of HMGB1 Attenuates Diabetic
- 40 Nephropathy in Mice. Sci Rep *8*, 8319. 10.1038/s41598-018-26637-5.
- 41. Zhou, B., Li, Q., Wang, J., Chen, P., and Jiang, S. (2019). Ellagic acid attenuates streptozocin
- induced diabetic nephropathy via the regulation of oxidative stress and inflammatory
- 43 signaling. Food Chem Toxicol *123*, 16-27. 10.1016/j.fct.2018.10.036.
- 44 42. Zhang, J., Yang, X., Zhang, X., Lu, D., and Guo, R. (2021). Electro-Acupuncture Protects

- Diabetic Nephropathy-Induced Inflammation Through Suppression of NLRP3 Inflammasome in Renal Macrophage Isolation. Endocr Metab Immune Disord Drug Targets *21*, 2075-2083. 10.2174/1871530321666210118161721.
- 4 43. Jin, J., Gong, J., Zhao, L., Zhang, H., He, Q., and Jiang, X. (2019). Inhibition of high mobility group box 1 (HMGB1) attenuates podocyte apoptosis and epithelial-mesenchymal transition by regulating autophagy flux. J Diabetes *11*, 826-836. 10.1111/1753-0407.12914.
- 8 44. Zhang, Y. (2021). MiR-92d-3p suppresses the progression of diabetic nephropathy renal fibrosis by inhibiting the C3/HMGB1/TGF-β1 pathway. Biosci Rep *41*. 10.1042/bsr20203131.
- 45. Aruffo, A., Stamenkovic, I., Melnick, M., Underhill, C.B., and Seed, B. (1990). CD44 is the
 principal cell surface receptor for hyaluronate. Cell *61*, 1303-1313. 10.1016/0092 8674(90)90694-a.
- 46. Goodison, S., Urquidi, V., and Tarin, D. (1999). CD44 cell adhesion molecules. Mol Pathol
 52, 189-196. 10.1136/mp.52.4.189.
- 16 47. Chan, G.C., Eng, D.G., Miner, J.H., Alpers, C.E., Hudkins, K., Chang, A., Pippin, J.W., and Shankland, S.J. (2019). Differential expression of parietal epithelial cell and podocyte extracellular matrix proteins in focal segmental glomerulosclerosis and diabetic nephropathy. Am J Physiol Renal Physiol *317*, F1680-f1694. 10.1152/ajprenal.00266.2019.
- Segade, F. (2010). Molecular evolution of the fibulins: implications on the functionality of the elastic fibulins. Gene *464*, 17-31. 10.1016/j.gene.2010.05.003.
- Tsai, Y.C., Hung, W.W., Chang, W.A., Wu, P.H., Wu, L.Y., Lee, S.C., Kuo, M.C., and Hsu, Y.L.
 (2021). Autocrine Exosomal Fibulin-1 as a Target of MiR-1269b Induces Epithelial Mesenchymal Transition in Proximal Tubule in Diabetic Nephropathy. Front Cell Dev Biol
 9, 789716. 10.3389/fcell.2021.789716.
- Scholze, A., Bladbjerg, E.M., Sidelmann, J.J., Diederichsen, A.C., Mickley, H., Nybo, M.,
 Argraves, W.S., Marckmann, P., and Rasmussen, L.M. (2013). Plasma concentrations of
 extracellular matrix protein fibulin-1 are related to cardiovascular risk markers in chronic
 kidney disease and diabetes. Cardiovasc Diabetol 12, 6. 10.1186/1475-2840-12-6.
- 30 51. Paudel, Y.N., Shaikh, M.F., Chakraborti, A., Kumari, Y., Aledo-Serrano, Á., Aleksovska, K., Alvim, M.K.M., and Othman, I. (2018). HMGB1: A Common Biomarker and Potential Target for TBI, Neuroinflammation, Epilepsy, and Cognitive Dysfunction. Front Neurosci *12*, 628. 10.3389/fnins.2018.00628.
- 34 52. Magna, M., and Pisetsky, D.S. (2014). The role of HMGB1 in the pathogenesis of inflammatory and autoimmune diseases. Mol Med *20*, 138-146. 10.2119/molmed.2013.00164.
- Wang, Y., Jiang, Z., Yan, J., and Ying, S. (2019). HMGB1 as a Potential Biomarker and Therapeutic Target for Malignant Mesothelioma. Dis Markers *2019*, 4183157. 10.1155/2019/4183157.
- 40 54. Rayego-Mateos, S., Morgado-Pascual, J.L., Opazo-Ríos, L., Guerrero-Hue, M., García-41 Caballero, C., Vázquez-Carballo, C., Mas, S., Sanz, A.B., Herencia, C., Mezzano, S., et al. 42 (2020). Pathogenic Pathways and Therapeutic Approaches Targeting Inflammation in 43 Diabetic Nephropathy. Int J Mol Sci *21*. 10.3390/ijms21113798.
- 44 55. Li, J., Ren, H., Wang, J., Zhang, P., and Shi, X. (2021). Extracellular HMGB1 promotes CD44

1	expression in hepatocellular carcinoma via regulating miR-21. Aging (Albany NY) 13
2	8380-8395. 10.18632/aging.202649.

- 3 56. Perez-Riverol, Y., Bai, J., Bandla, C., García-Seisdedos, D., Hewapathirana, S., Kamatchinathan, S., Kundu, D.J., Prakash, A., Frericks-Zipper, A., Eisenacher, M., et al. (2022). The PRIDE database resources in 2022: a hub for mass spectrometry-based proteomics evidences. Nucleic Acids Res *50*, D543-d552. 10.1093/nar/gkab1038.
- 7 57. Xiao, L., Xu, X., Zhang, F., Wang, M., Xu, Y., Tang, D., Wang, J., Qin, Y., Liu, Y., Tang, C., et al. (2017). The mitochondria-targeted antioxidant MitoQ ameliorated tubular injury mediated by mitophagy in diabetic kidney disease via Nrf2/PINK1. Redox Biol *11*, 297-10 311. 10.1016/j.redox.2016.12.022.

11

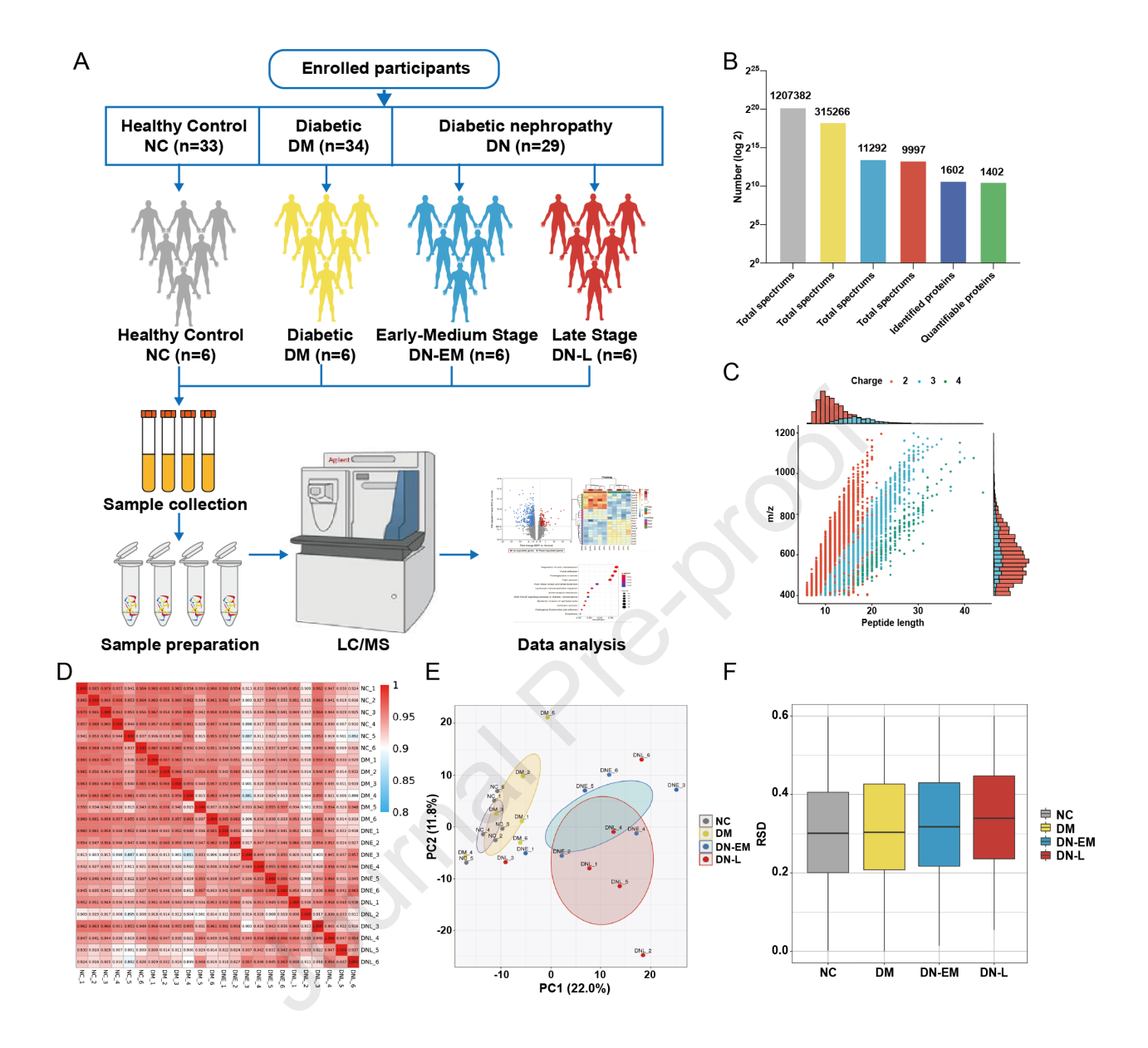
Table 1. Demographic Characteristics of the Participants

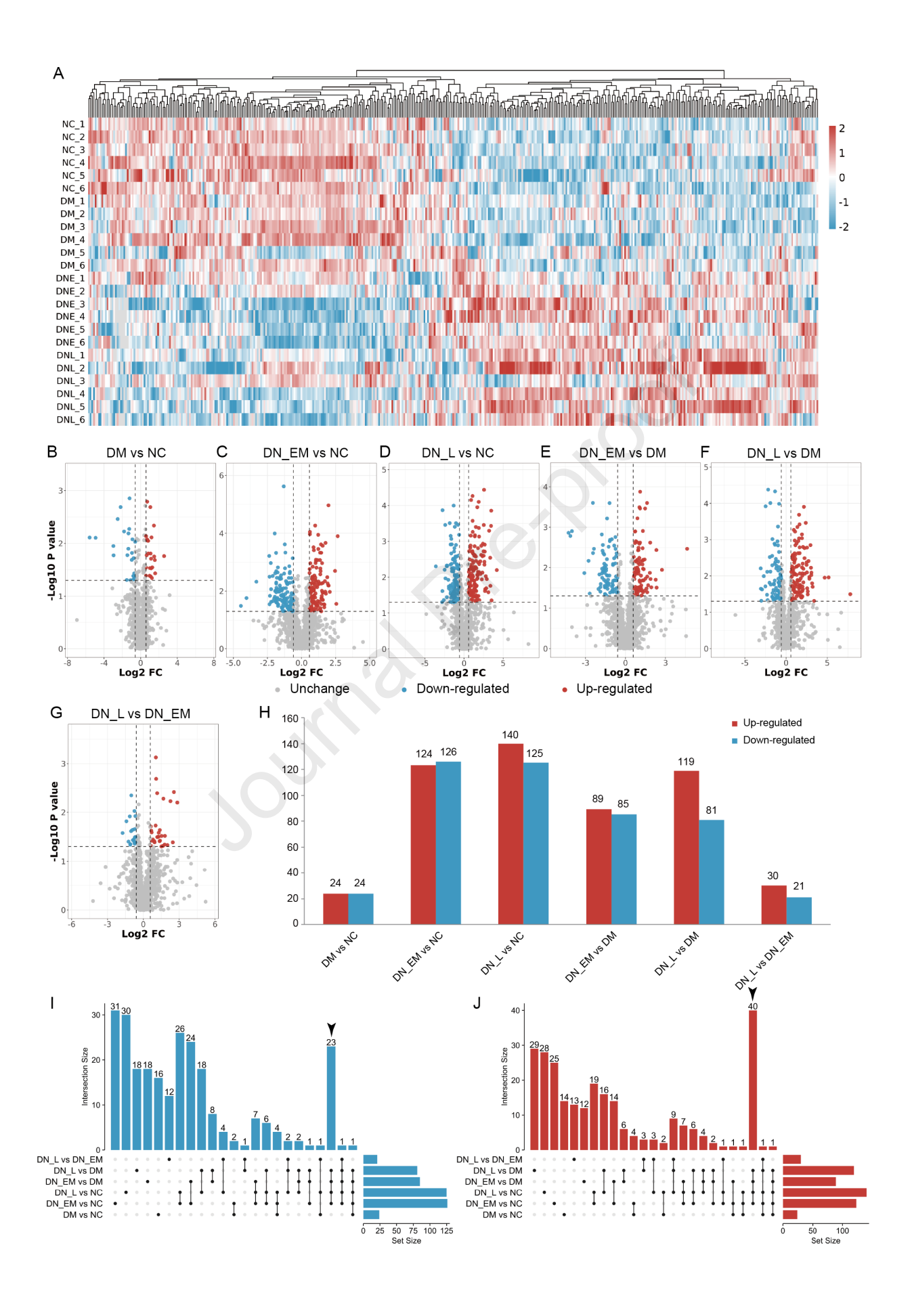
	1461011 201	nographic Character	istics of the fulfile	Punts	
Variable	NC	DM	DN-EM	DN-L	P
variable	(N=6)	(N=6)	(N=6)	(N=6)	Γ
Age	51.50±5.01	48.17±5.04	63.83±12.98 ^b	63.50±8.31 ^b	0.007~
(Years)	31.30±3.01	46.17±3.04	03.83±12.98	03.30±8.31	0.007~
Gender	4/2	2/4	4/2	2/4	0.541#
(Female /Male)	4/2	2/4	4/2	2/4	0.541#
eGFR	99.57±5.68	102.06±7.43	63.67±15.04 ^{ab}	18.89±9.38 ^{abc}	<0.001~
(ml/min/1.73m2)	99.37±3.08	102.00±7.43	03.07±13.04**	18.89±9.36***	<0.001∼
Glu (mmol/L)	4.47 (4.14-4.72)	7.59 (6.02-10.08) ^a	6.68 (5.99-13.66) ^a	8.6 (5.35-11.58) ^a	0.010*
BUN (mmol/L)	5.12±1.45	5.00±1.37	6.29±2.26	10.06 ± 1.76^{abc}	<0.001~
SCr (µmol/L)	57.5 (47.25-63.75)	54.0 (48.00-60.75)	67 (62.00-116.25)	180 (177.25-396.25) ab	0.001*
BUN/SCr	0.085 (0.075-0.115)	0.09 (0.068-0.118)	0.09 (0.083-0.090)	0.04 (0.028-0.055) ab	0.009*
Cys-C (mg/L)	0.85 (0.79-0.89)	0.84 (0.77-0.89)	1.16 (1.05-2.07)	3.27 (2.24-5.42) ab	<0.001*
UA (μmol/L)	276.5 (216.75-313.50)	250.0 (228.00-411.75)	335 (235.50-359.50)	414 (289.00-429.75)	0.283*

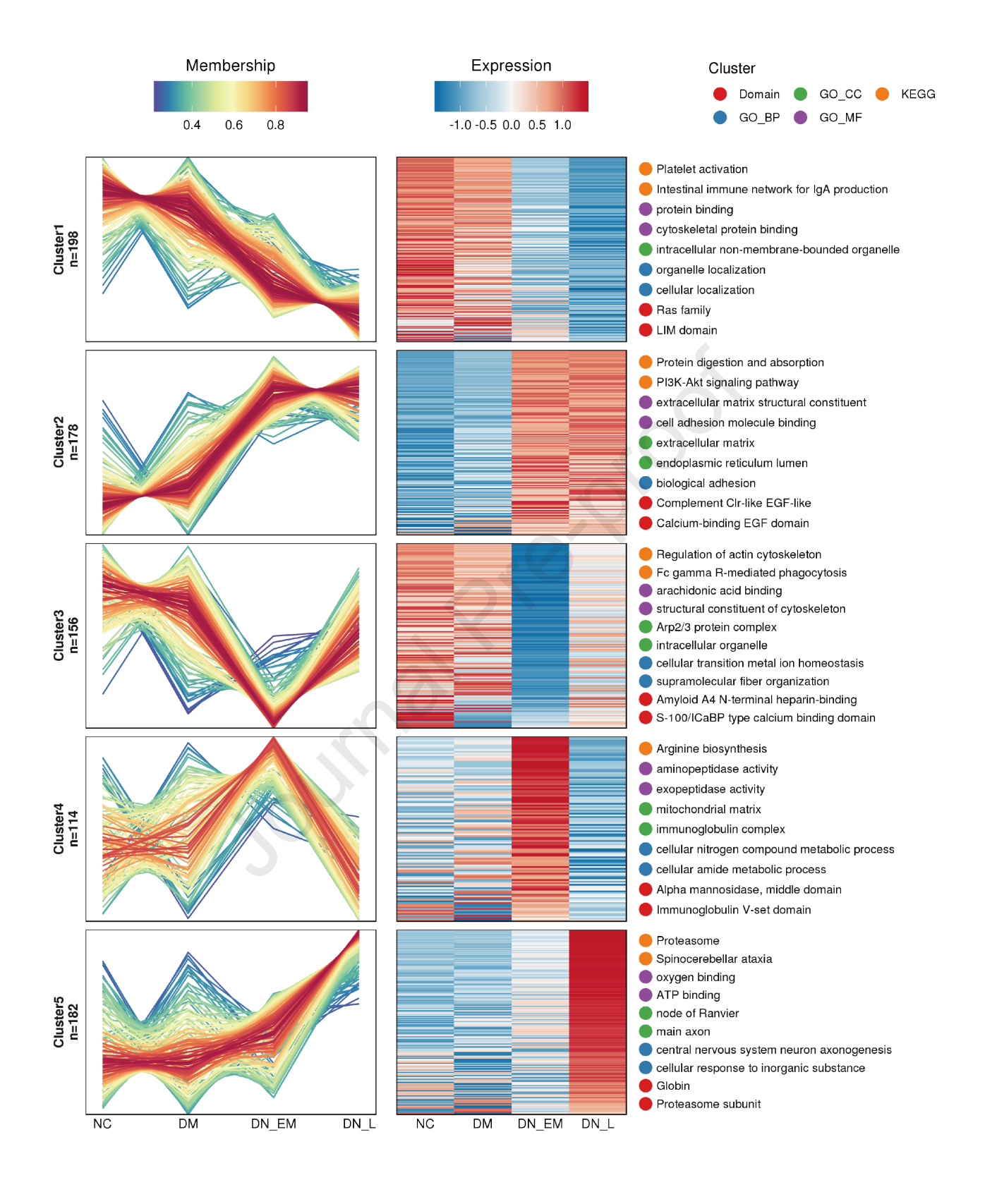
eGFR: estimated glomerular filtration rate; Glu: glucose; BUN: blood urea nitrogen; SCr: serum creatinine; BUN/ Scr; blood urea uitrogen to serum creatinine ratio; Cys-C: cystatin c; UA: uric acid; ~: Analysis of variance (ANOVA); #: Fisher's Exact Test; *: Kruskal-Wallis Test; $^aP < 0.05$ vs NC group; $^bP < 0.05$ vs DM group; $^cP < 0.05$ vs DNEM group.

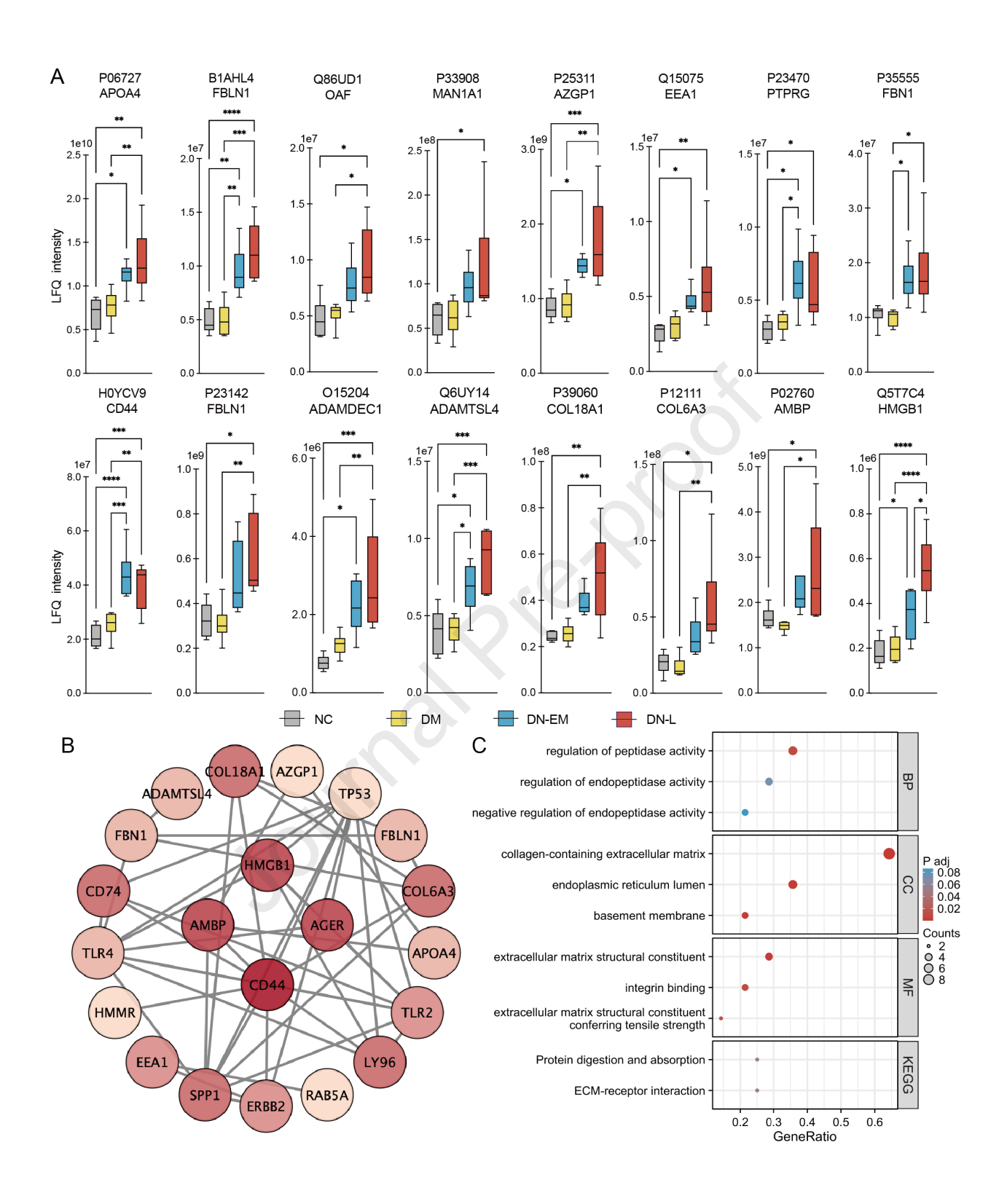
Table2. The basic information of shared proteins between MEblue and Cluster2

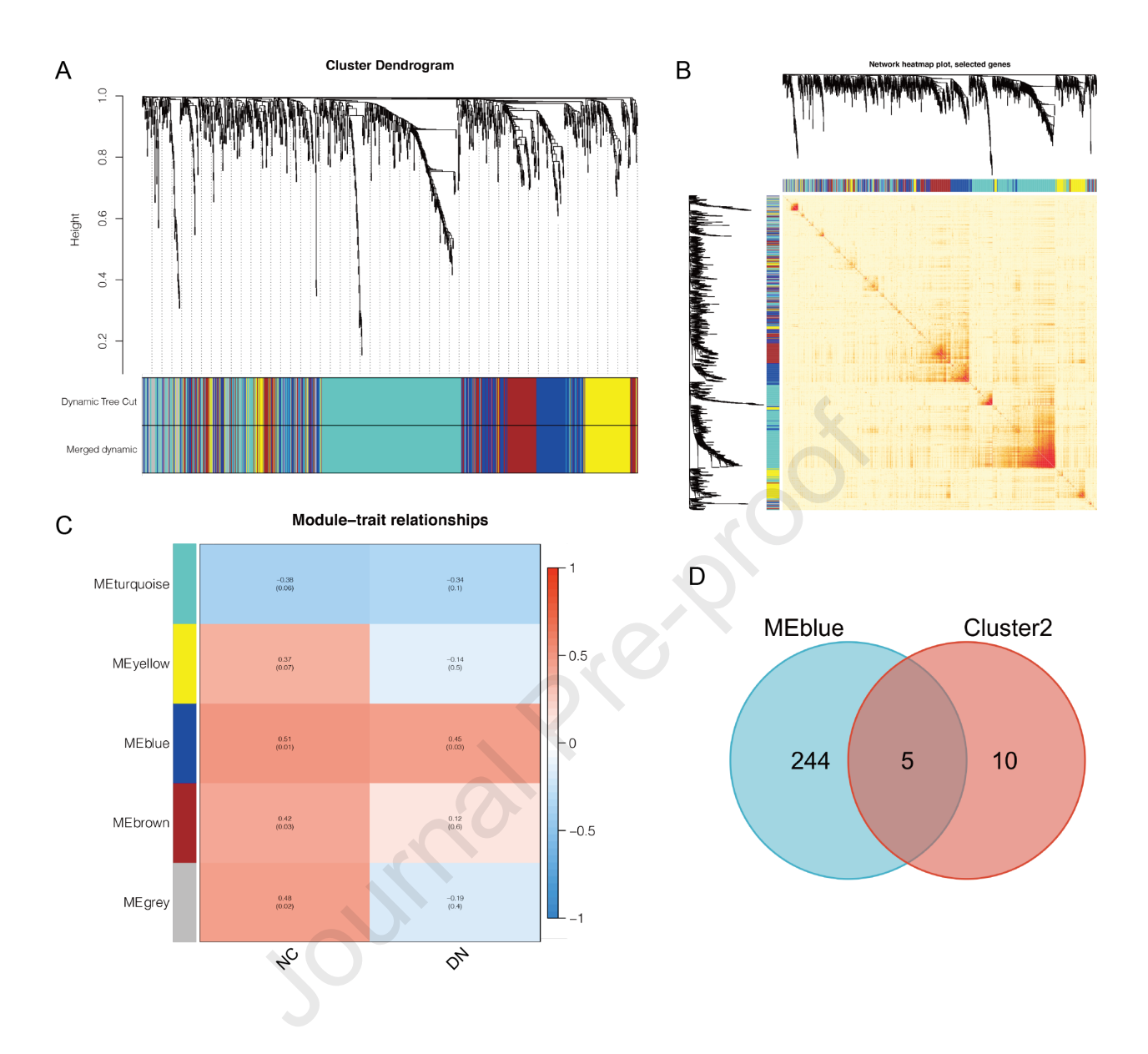
Protein accession	Protein description	Gene name	Subcellular locations from UniProtKB/Swiss-Prot	Relevance scores from Genecards
Q5T7C4	High mobility group protein B1	HMGB1	Nucleus. Chromosome. Cytoplasm. Secreted. Cell membrane. Peripheral membrane protein. Extracellular side. Endosome. Endoplasmic reticulum-Golgi intermediate compartment. Endoplasmic reticulum.	10.5875282287598
H0YCV9	CD44 antigen	CD44	Cell membrane. Single-pass type I membrane protein. Cell projection, microvillus.	6.28472328186035
B1AHL2/ P23142	Fibulin-1	FBLN1	Secreted, extracellular space, extracellular matrix.	2.0302460193634
P23470	Receptor-type tyrosine- protein phosphatase gamma	PTPRG	Membrane. Single-pass type I membrane protein.	None
Q6UY14	ADAMTS-like protein 4	ADAMTSL4	Secreted, extracellular space, extracellular matrix.	None

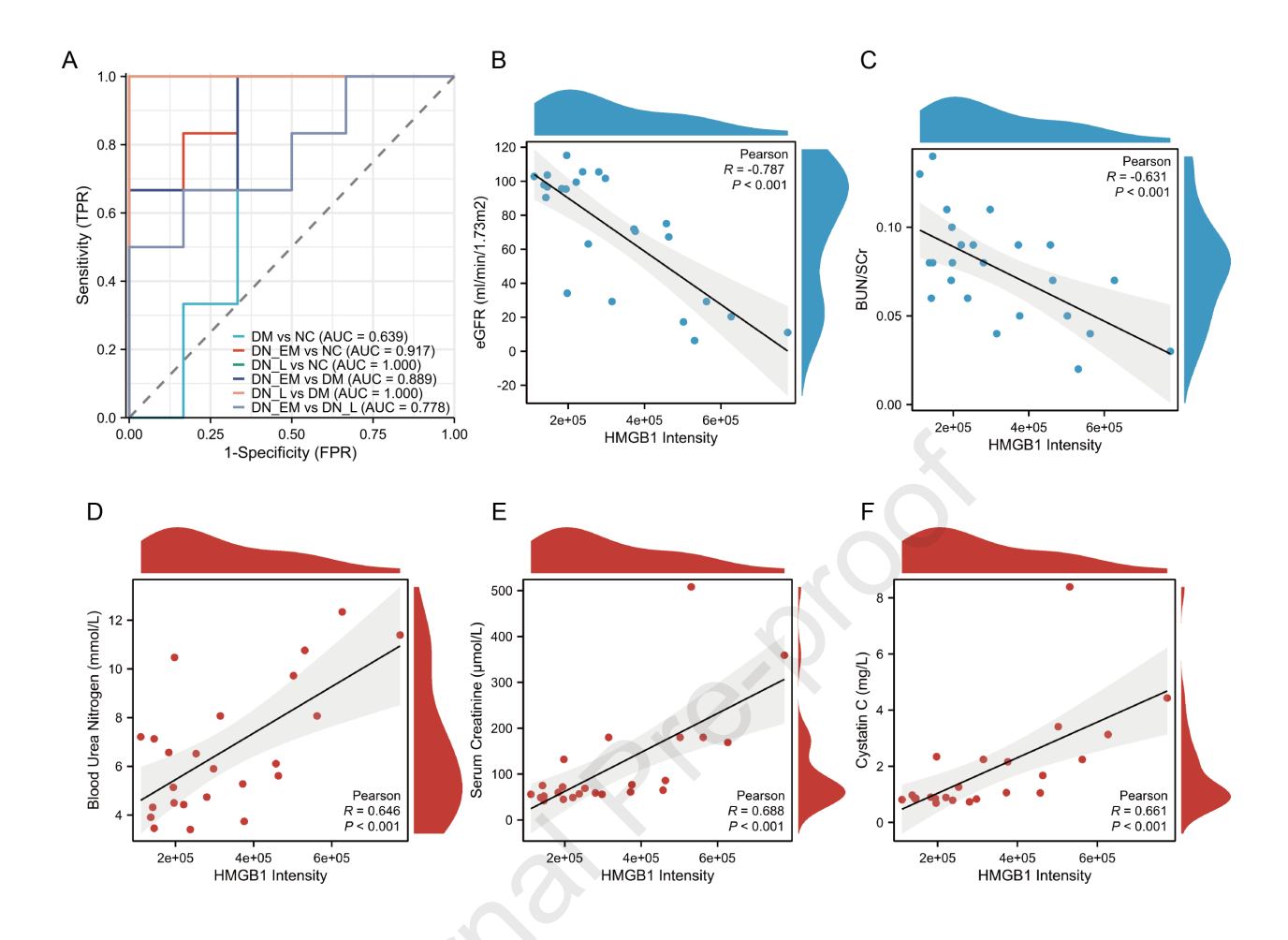


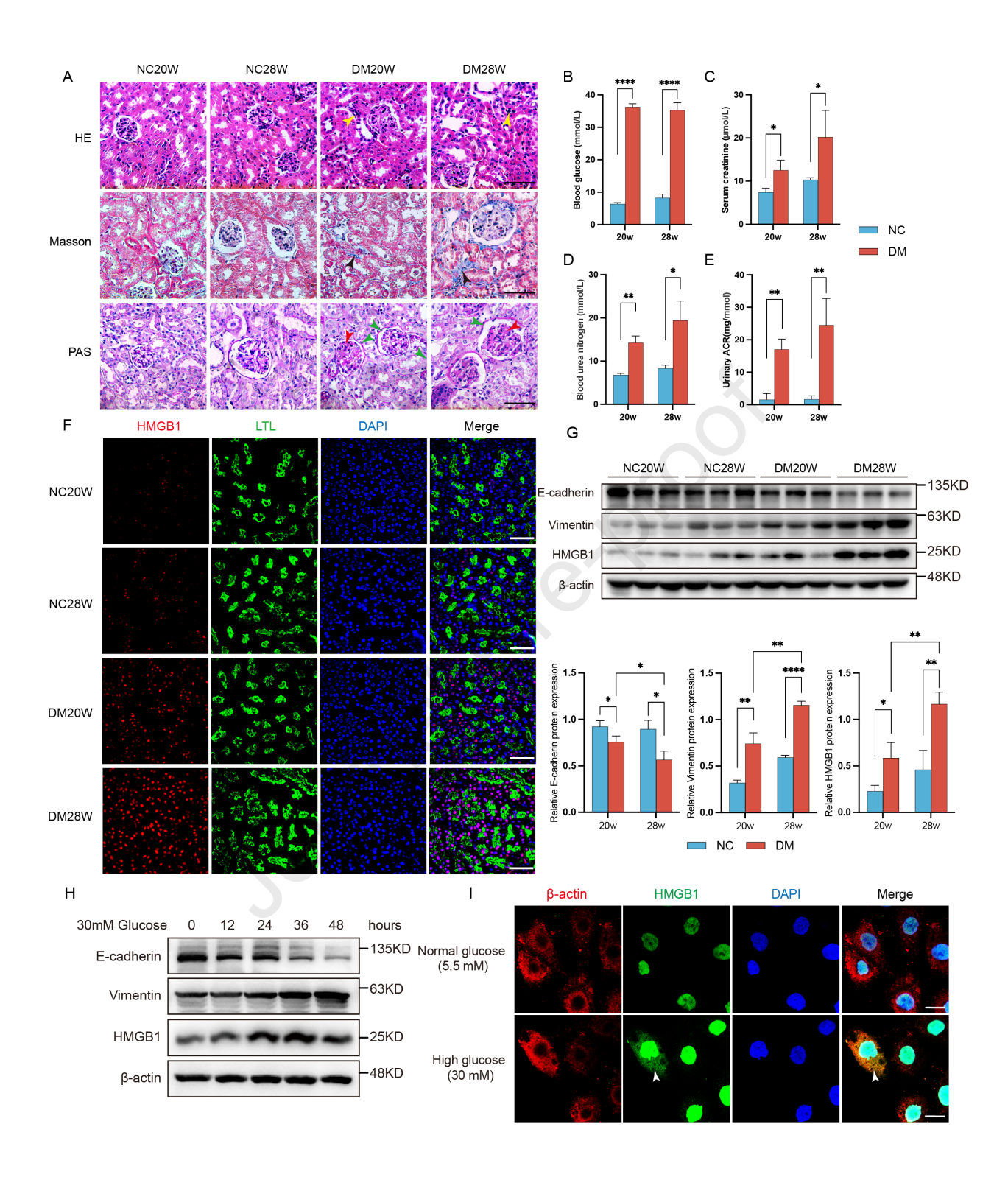












Highlights

- Potential biomarkers increased along with diabetic nephropathy progression
- HMGB1 as an acceptable biomarker for the early monitoring of diabetic nephropathy
- HMGB1 was elevated under high glucose conditions both in cells and animals

KEY RESOURCES TABLE

REAGENT or RESOURCE	SOURCE	IDENTIFIER
Antibodies		
Anti-HMGB1	Abcam	ab79823;
		RRID:AB_1603373
Anti-E-cadherin	Proteintech	20874-1-AP;
		RRID:AB_10697811
Anti-Vimentin	Proteintech	10366-1-AP;
		RRID:AB_2273020
Anti-β-actin	Proteintech	66009-1-Ig;
		RRID:AB_2687938
Anti-rabbit IgG, HRP-linked Antibody	Cell Signaling Technology	7074;
		RRID:AB_2099233
Anti-mouse IgG, HRP-linked Antibody	Cell Signaling Technology	7076;
		RRID:AB_330924
Lotus tetragonolobus lectin (LTL)	Vector Laboratories	B-1325;
		RRID:AB_2336558
FITC Goat Anti-Rabbit IgG (H+L) Antibody	ApexBio Technology	K1203
Cy3 Goat Anti-Mouse IgG (H+L) Antibody	ApexBio Technology	K1207
Cy3 Goat Anti-Rabbit IgG (H+L) Antibody	ApexBio Technology	K1209
Biological samples		
Serum samples from patients	Affiliated Hospital of	This paper
	Guizhou Medical University	
Chemicals, peptides, and recombinant proteins	S	
Streptozotocin (STZ)	Solarbio	S8050
Dulbecco's modified Eagle's/F12 medium	Gibco	C11330500BT
Fetal bovine serum	Gibco	2497736
D-glucose	Solarbio	G8150
phenylmethanesulfonyl fluoride (PMSF)	Solarbio	P0100
Enhanced chemiluminescence reagents	Absin	abs920
Critical commercial assays		
Pierce™ Top 12 Abundant Protein Depletion	Thermo Fisher scientific	85164
Spin Columns Kit		
BCA Protein Assay Kit	Beyotime	P0011
Hematoxylin and eosin staining Kit	Solarbio	G1220
Masson trichrome staining Kit	Solarbio	G1346
Periodic acid-schiff staining Kit	Solarbio	G1281
Deposited data		
Mass spectrometry data	ProteomeXchange	PXD047872
Experimental models: Cell lines	ı	

HK-2 cells	Procell Life	Cat# CL-0109;
	Science&Technology	RRID:CVCL_0302
Experimental models: Organisms/strains	S	
C57BL/6	Charles River	RRID:MGI:2159769
Software and algorithms		
STRING	N/A	http://string-db.org
		RRID:SCR_005223
Cytoscape (version 3.9.1)	Open source	https://cytoscape.org
		RRID:SCR_003032
GraphPad Prism	GraphPad Software	RRID:SCR_002798
ImageJ	National Institutes of Health	RRID:SCR_003070
R (version 4.2.1)	R Project	https://www.r-
		project.org
SPSS 26.0	IBM	RRID:SCR_002865
Other	40	
polyvinylidene difluoride (PVDF)	Millipore	ISEQ00010
membranes		